Journal of Aircraft

VOLUME 1 MARCH–APRIL 1964 NUMBER 2

27th Wright Brothers Lecture

Some Opportunities for Progress in Aircraft Performance

GEORGE S. SCHAIRER
The Boeing Company, Seattle, Wash.

An examination of aerodynamic and propulsion fundamentals shows where research might result in significant progress in aircraft performance. Turbulent skin friction can be reduced by delayed transition, damping, and other forms of boundary-layer control. Separation control by both proper shaping and by boundary-layer control will improve C_D at high C_L and maximum C_L. Research at transonic Mach numbers on two-dimensional airfoils will give higher practical values of M^2C_L. This leads to lower drag of swept wings at supersonic speeds. Lift and propulsion by yawed propellers and helicopter rotors show untapped performance potential. The propulsive efficiency of ducted fans can be improved. Design point gas generator performance is subject to much improvement from higher temperatures, higher pressures, regeneration, and reheat. Variable airflow compressors, fans, and turbines will provide large improvements at off-design conditions. Aircraft requiring V/STOL or low-altitude cruise, or supersonic cruise, or high speed at sea level will benefit from multiple design point engines. Current powered lift schemes for V/STOL can be improved in transition. Ground effects have much room for improvement. In conclusion, large improvements in ceiling, speed, range, low speed, endurance, low-altitude performance, and supersonic range are possible.

Nomenclature

A = wing aspect ratio
b = span, ft
b_e = effective span, ft
C_D = drag coefficient, D/qS
C_L = lift coefficient, L/qS
C_L''' = wing lift coefficient referred to slipstream dynamic pressure
C_{Di} = induced drag coefficient, $C_L^2/\pi A$
C_f = skin friction coefficient, τ_0/q
C_Q = flow quantity coefficient = air mass flow/ρVS
C_T = thrust coefficient, T/qS
C_μ = jet flap momentum coefficient = jet momentum flux/qS
C_V = nozzle velocity coefficient = actual velocity/ideal velocity
c = chord, ft
d = propeller or rotor diameter, ft
D = drag or force parallel to flight path (positive when it tends to retard motion), lb
q = acceleration of gravity, 32.2 ft/sec^2
H = stream total head, psf
L = lift or force normal to flight path, lb
M = Mach number
M_L = local Mach number
N = rotational speed, rpm
P = pressure, psf
P = power required
P_0 = power required in hovering out of ground effect
P_S = static pressure, psf
P_2 = total pressure at compressor face, psf
P_3 = total pressure at compressor outlet, psf
P_7 = total pressure at tailpipe, psf
P_{AM} = ambient pressure, psf
q = dynamic pressure based on forward flight velocity, psf
q'' = dynamic pressure based on slipstream velocity, psf
q_t = dynamic pressure based on rotational tip velocity, psf
R = rotor radius, ft
R_δ = Reynolds number = $U_0\delta/\nu$
S = wing area, ft^2
s = slot width
SFC = specific fuel consumption, lb fuel/hr/lb thrust
T = thrust or force produced by propulsion system irrespective of direction, lb
T_C'' = thrust coefficient based on slipstream dynamic pressure
T_2 = total temperature at compressor face, °R
T_5 = total temperature at turbine, °R
T_7 = tailpipe total temperature, °R
T_{AM} = ambient temperature, °R
u = perturbation velocity, fps
u_L = velocity at edge of boundary layer, fps
U_0 = freestream velocity, fps
V = flight velocity, fps or knots
V_j = computed jet velocity assuming isentropic expansion from duct pressure to remote static
V_t = rotor blade rotational tip velocity, fps
W = aircraft weight, lb

Presented at the AIAA Aerospace Sciences Meeting, New York, January 20, 1964. The author was assisted in the preparation of this paper by Jim Foody, Wayne Wiesner, Tom Lollar, and Ed Farris, and with the assistance of Frank Davenport, John Acurio, Gordon Lampard, Frank Harris, Maury Young, and Walt Blissell.

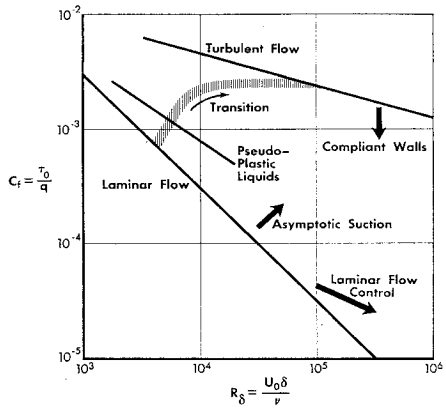

Fig. 1 Local boundary-layer friction vs Reynolds number based on boundary-layer thickness.

W_a = airflow, lb/sec
W_f = fuel flow, lb/hr
α = angle of attack, deg
γ = specific heat ratio = 1.4
δ = boundary-layer thickness, ft
δ_2 = total pressure ratio at compressor face
δ_{AM} = ambient pressure ratio
η = efficiency
η_c = compressor adiabatic efficiency
η_p = propulsive efficiency
η_t = thermal efficiency
θ_2 = total temperature ratio at compressor face, $T_2/519$
θ_{AM} = ambient temperature ratio, $T_{AM}/519$
Λ = wing sweep angle, deg
ν = viscosity, ft²/sec
ρ = air density, slug/ft³
τ_0 = local shear stress at wall, psf
ω = angular velocity, rad/sec

THE Wright brothers' flight of December 17, 1903 climaxed many years of engineering research and engineering design by the Wright brothers. This engineering research and design process has continued in the 60 years following their first flight, with many thousands of talented people applying their best efforts to the process. This paper will take a look at some of the opportunities that remain 60 years later for further progress in the art of engineering research and design, as applied particularly to the area of aircraft performance. "Aircraft performance" is defined for the purpose of this paper as that combination of powerplant and aircraft performance that gives the over-all performance of the aircraft. This paper is confined to aircraft flying within the atmosphere and propelled by air-breathing power plants. Time and space do not permit including the very important subject of the aircraft empty weight.

"Progress" is defined in the dictionary as "movement forward; onward course; progression; advance to an objective; a going or getting ahead." On the basis of past accomplishments in aeronautical research and aircraft design, a springboard exists from which progress can be made toward new and better designs, as well as new and more satisfactory research explanations of the processes involved in flight. This paper will list some of these opportunities for progress in aircraft performance in the hope that focusing attention on them will cause the initiation of additional research or the application of available research to new aircraft designs.

Compressible Aerodynamics

In the preparation of this paper, one particular problem has repeatedly plagued analyses: compressible vs incompressible aerodynamics. Nearly all the literature on the lift and drag characteristics of bodies is written in the context of incompressible aerodynamics. Only from about 1940 onward was compressibility generally included in aerodynamics—largely by the addition of the term Mach number. This was done without much reversion back to the fundamental processes of the flow. The concept of dynamic pressure $q = \frac{1}{2}\rho V^2$ has been exceedingly useful in subsonic low Mach number aerodynamics. The concept of q has little practical value at high subsonic Mach numbers and higher velocities. As a first step toward bringing compressible aerodynamics into low-speed calculations of flight, it is convenient to use the term $q = \frac{1}{2}\rho V^2 = (\gamma/2)P_S M^2$.

Modern aircraft design seldom can be limited to incompressible aerodynamics, since the tips of the propulsion systems are nearly always operating at about the speed of sound. This is true of the tips of helicopter rotors, as well as powerplant fans, and it is certainly true of the compressors and turbines of the gas turbines that propel modern aircraft. Thus, it is not possible to describe powerplant performance without using compressible aerodynamics and a proper transfer between the airplane aerodynamics; and the powerplant aerodynamics is not possible unless they are both expressed in compressible terms. This requires the $(\gamma/2)P_S M^2$ definition for q. The common use of this alternate definition for q will certainly assist materially in making research and design analyses. Probably, however, this is only the first step that can and should be taken toward a progress in aerodynamic terminology. Possibly, aerodynamic sshould be related to total head

$$H = P_S\left(1 + \frac{\gamma - 1}{2} M^2\right)^{\gamma/(\gamma - 1)}$$

or $H - P_S$ rather than q.

Opportunity 1

Progress in aircraft performance will be accelerated by conversion to compressible aerodynamic terminology.

Skin Friction

The principal source of drag losses in both aircraft and engine design is the viscous skin friction of the air flowing over the aerodynamic surfaces. Aerodynamicists continue to search for better definitions of viscous skin friction and, in particular, for ways to reduce it. Figure 1 is a plot of local skin friction coefficient $C_f = \tau_0/q$ vs Reynolds number R_δ based upon boundary-layer thickness. A number of opportunities have been proposed for reducing the viscous skin friction. There is little indication in the literature of any hope for bettering the laminar skin friction curve.

Many years ago, Eastman Jacobs and his associates at NACA showed that the use of smooth surfaces and especially designed airfoils that gave favorable pressure gradients would permit the delay of transition and, hence, the attainment of very low friction coefficients on the areas where a thick laminar boundary layer grew naturally. Because of the surface roughness problem, few attempts have been made by these means to obtain laminar flow on practical aircraft. Pfenninger[1] and his associates at Northrup are working on the use of suction slots to delay transition. They have built the X-21 aircraft as part of their program. These suction slots do not prevent growth of the boundary layer and do not result in any asymptotic boundary-layer condition, but rather are intended to stabilize the boundary layer while allowing it to thicken, and thus obtain the low friction coefficients that come at high Reynolds numbers. It is not obvious from theory or experiment how far one can go with this process but successes to date are very encouraging, both with respect to the stabilization that has been accomplished and the practical methods that have been developed for accomplishing this stabilization.

The use of extensive suction to attain constant boundary-layer thickness, and thus keep the Reynolds number of the laminar flow to a fixed value, should be studied further; how-

ever, extensive suction involves large pumping losses and keeps the boundary layer quite thin where surface roughness can cause transition.

In recent years there has been much discussion of compliant walls[2] which might change the flow processes in the turbulent flow region, or possibly in the transition region. Inasmuch as there is no satisfactory mathematical definition of either the turbulent flow processes or the transition process, no satisfactory theory of compliant walls has been possible. A number of experiments have been conducted on compliant walls with various objectives in mind, such as a damping of certain particular frequencies that might be important in energy dissipation or that might be the cause of transition. Continued theoretical and experimental work in this area should be encouraged. So little is known about the nature of turbulent boundary layers, and so much benefit would accrue to aviation from a reduction in turbulent skin friction, that all avenues for its reduction should be thoroughly examined.

The aeronautical engineer must be careful to remember at all times that the expressions presented on Fig. 1 are only man's explanation of the flow processes, and big surprises can lie immediately at hand. Two examples demonstrate the inadequacies of Fig. 1 as an expression of our understanding of the true flow processes. The conventional definition of fluid skin friction involves forces that are assumed to be proportional to the shear gradient. These are fluid where the viscous shear is not proportional to the shear gradient and these fluids have turbulent skin frictions far below the values for air. References 3 and 4 describe some pseudo-plastic fluids which have lower turbulent frictions, as shown on Fig. 1. Another familiar example of the inadequacies of Fig. 1 and the limitations of incompressible aerodynamics is the skin friction at high Mach numbers where the boundary layer is self-heated. The air viscosity changes with temperature and, hence, the viscous shear forces vary across the boundary layer.

Many experiments have been conducted with light gases injected into the boundary layer as a means for reducing skin friction. Possibly the introduction of molecules that would make the air behave like a pseudo-plastic is possible. All such opportunities should be researched thoroughly.

Opportunity 2

Many opportunities exist for the aeronautical researcher, theoretically and experimentally, to understand, and possibly to reduce, turbulent skin friction drag and delay transition. The application of laminar flow control by suction slots to a production prototype aircraft appears to be timely.

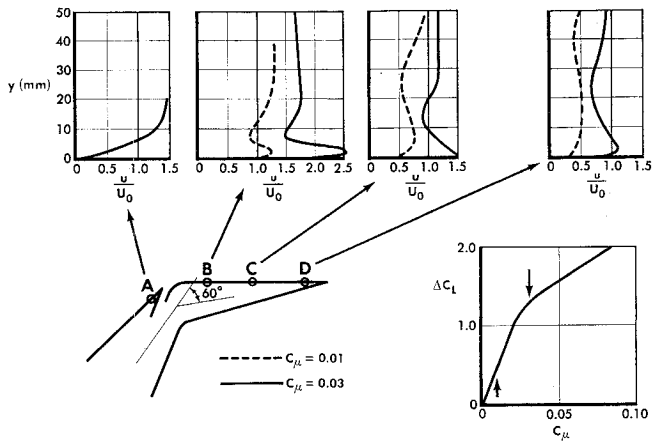

Fig. 2 Boundary-layer velocity profiles on deflected flap for different blowing coefficients.

Flap Boundary-Layer Control

Since about 1928, when flaps were first used, a substantial portion of flap research has been devoted to means for preventing separation of the air from the upper surface of the flap. Slots between the wing and flap have been used extensively to minimize the upper surface separation and to provide flow more nearly matching potential nonviscous attached flow. In Ref. 5, Carriere, Eichelbrenner, and Poisson-Quinton presented a rational engineering approach to blowing over the flap in such a way as to cause the air flow to adhere on the upper surface. Figure 2 shows typical boundary-layer profiles with jet augmentation. It was shown by Carriere, et al., that two regions of lift augmentation exist with varying $C\mu$. The first region is that in which the flow over the upper surface of the flap is caused to adhere and approach potential flow. The second region is one in which the jet of air causes a jet flap effect. Carriere, et al., showed that the amount of blowing required at the transition between these two regions would just correct the total head deficiency at the surface of the flap at the trailing edge. It is not necessary to replace the total momentum deficiency of the boundary layer to accomplish essentially potential flow-lift coefficients. This work suggests that, as a first approximation, flap blowing systems can be designed experimentally either in the wind tunnel or in free flight by the use of total head rakes at various places along the flap trailing edge and by the adjustment of the blowing flow until the total head deficiency at the surface of

---

George S. Schairer

George S. Schairer is the Vice-President—Research and Development of The Boeing Company. Born in Wilkinsburg, Pennsylvania in 1913, he graduated from Swarthmore College with a B.S. degree in 1934 and from Massachusetts Institute of Technology with an M.S. degree in 1935. He was employed by the Bendix Products Corporation in South Bend, Indiana and Consolidated Aircraft (now General Dynamics) in San Diego prior to joining Boeing in 1939 as head of the Aerodynamics Unit. He has held the positions of Staff Engineer—Aerodynamics and Power Plant, Chief of Technical Staff, Assistant Chief Engineer, and Director of Research. He has participated in the aerodynamic design of such Boeing airplanes as the Stratoliner, B-17, B-29, B-50, XPBB-1, C-97, Stratocruiser, B-47, B-52, 707, and the KC-135.

He is a Fellow and Technical Director of the American Institute of Aeronautics and Astronautics. He has received the Sylvanus Albert Reed award of the Institute of Aerospace Sciences and the Spirit of St. Louis Medal of the American Society of Mechnical Engineers. He holds an honorary Doctor of Engineering degree from Swarthmore College.

Dr. Shairer has written numerous papers in the field of aircraft design and aerodynamics. He has twice served as a member of the U. S. Air Force Scientific Advisory Board. He has been a consultant to the Director of Defense, Research and Engineering and is a member of the U. S. President's Science Advisory Committee, Panel on Scientific and Technical Manpower. He had served for many years on the NACA Aerodynamic Committee and also with NASA through 1960, along with numerous other technical committees.

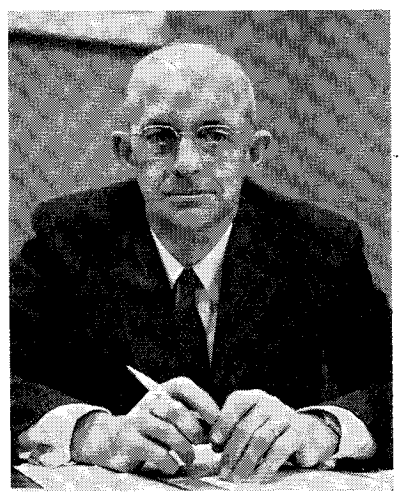

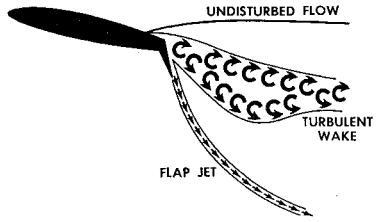

Fig. 3 Possible separation of the wake of a blown flap.

the flap is fully corrected. It appears that the engineering tools are now available for the design and application of blown flaps. With the advent of turbo machinery, pressurized air will readily be available to make very simple blown flaps a fundamental part of most future aircraft.

Opportunity 3

The design tools are now available for the successful application of blown flaps.

Blown Flap Separated Flow

Recent wind tunnel tests conducted at Stanford University and flight tests by Raspet, Cornish, and associates at Mississippi State University[6] showed that the blown flap problem is not quite so simple as would be indicated in the preceding section and that a large low-energy wake can exist behind blown flaps. In this circumstance the flow appears to be attached to the wing and also to the flap, but a large low-energy wake exists behind the flap in which the flow has very low velocity and, on occasion, probably has forward velocity. This is shown on Fig. 3. Presumably this low-energy flow or separation is a breakdown of the airflow above the jet-energized wake, and the condition of full total head augmentation at the trailing edge surface is not a complete and adequate definition of proper flow. The loss in energy in the air as it flows over the forward portion of the wing may very well be such that under some circumstances blowing at the flap leading edge cannot establish satisfactory flow. Stanford tests[7, 8] and also Williams, Butler, and Wood[9] have shown that at modest flap angles almost all of the blown flap jet momentum is recovered as forward thrust. At large flap angles the thrust recovery is reduced until it becomes zero near 90° flap deflection. Presumably this loss of thrust recovery also denotes a loss in jet flap effectiveness and general loss in lifting capability of the wing-flap combination. Apparently the loss in lift is never so great but that the large flap angles provide more lift than the small flap angles. It seems likely that, if the low-energy wake were cured by proper blowing, leading edge devices, or other upper surface treatment, the wing would have greater lift and would approach 100% recovery of blown jet momentum. Under these circumstances the only significant source of drag available to cause a rate of descent in a blown or jet flap airplane would be induced drag, since all of the momentum would appear as a thrust. As just shown, this thrust probably need not exceed skin friction drag. Further exploration of this phenomenon of jet flap separation appears urgent.

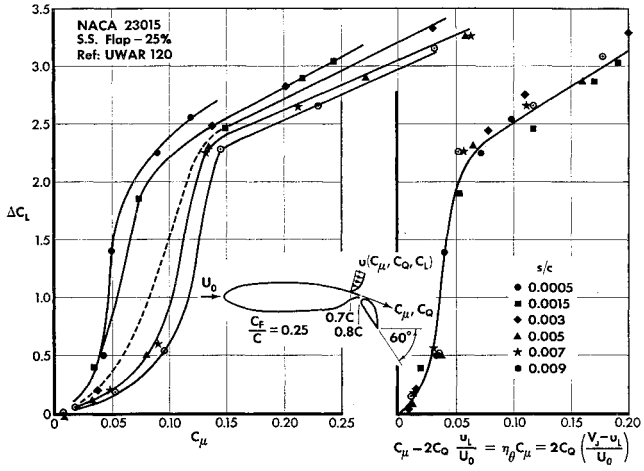

Fig. 4 Correlation of lift data using momentum coefficients based on a) freestream velocity and b) local velocity.

Opportunity 4

A requirement exists for a better understanding of separated and low-energy flows behind blown flapped wings.

Flap Blowing Requirements

It is common practice to assume that flap boundary-layer control is evaluated by the momentum coefficient C_μ of the air blown over the flap. Recently, theory[10, 11] and experiments have shown that a momentum efficiency must be used to represent adequately the actual flows. This theory and the experimental data show that the momentum which must be added must be based on the local velocity at the blowing point and not on the freestream velocity. A typical set of data[12] verifying this is shown on Fig. 4. The change in lift coefficient brought about by blowing on a flap is shown as a function of momentum coefficient C_μ for six different slot sizes and, hence, six different jet velocities. The same data are corrected to momentum based on local velocity. The coincidence of the data plotted to $\eta_\theta C_\mu$ is outstanding and suggests much merit to the theory. This shows that the higher the velocity, the lower the momentum required to stabilize the flow over the flap. Figure 4 suggests that slotted flaps which use ram air and, hence, produce velocities at the slot not greater than local freestream velocity, will be substantially less effective than an ordinary blown flap. No amount of freestream blowing appears to be the equivalent of higher energy jet blowing.

Opportunity 5

A theory exists to explain the blowing requirements of jet boundary-layer control flaps; it indicates that higher velocity blowing is far superior to that obtained in a slotted flap.

Leading-Edge Stalling

The lift coefficient vs angle-of-attack relationships for a two-dimensional airfoil with flaps up and with a large flap deflection are shown by the heavy lines on Fig. 5. The dotted lines on Fig. 5 are the lift vs angle-of-attack relationships that are predicted by potential flow theory. The principal deficiency in the flaps-up case is at the stall. In the flaps-down case only a little more than one-half the potentially available increment in lift from the flap is ordinarily obtained. In addition, an early stall is likely to occur in the flaps-down case. Flap boundary-layer control procedures, covered in the previous paragraphs, permit the attainment of flap-lift increments approaching potential flow values. Thus separation appears to have been removed as a principal unknown problem in the design of flaps. Flaps now can be understood and designed in terms of the potential flow predicted for them.

This suggests that the next attack on maximum lift coefficient should be directed toward delaying the leading edge

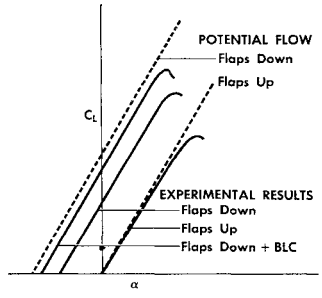

Fig. 5 Airfoil lift characteristics.

stall. Most research on leading edge stalling, and means to delay it, have been directed to such devices as slats, leading edge flaps, drooped noses, etc. Such mechanical leading edge devices have been adequate to meet the demands of the past; presumably for this reason little research has been directed to the fundamentals of leading edge stalling. With the advent of turbine machinery to provide boundary-layer control air, a new look and greatly increased attention appears appropriate to leading edge boundary-layer control and the fundamentals of stalling. References 13–17 cover some of the small bibliography available in this area. This material suggests that research on leading edge stalling, along the lines of that just reported on flap stalling, will probably lead to substantial improvements (see Fig. 6). The problem of leading edge stalling is not necessarily similar to or solvable by the same means that work for flap boundary-layer control. Reference 18 suggests that leading edge stalling may well be associated with a laminar rather than turbulent separation. Figure 7 shows the very unstable boundary layer at the leading edge and the extent to which this boundary layer was stabilized by transition-producing jets on the lower surface.

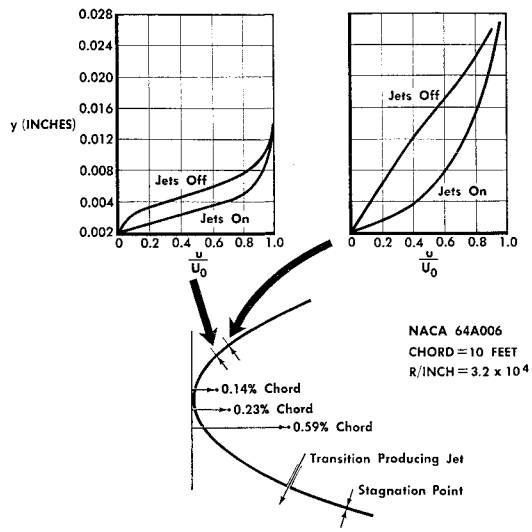

Fig. 7 The effect of transition on velocity profiles near the leading edge.

Opportunity 6

Aerodynamic research applied to delaying leading edge stall is likely to produce very large increases in stall angle and $C_{L_{max}}$.

Subsonic Airfoils

In 1940 Eastman Jacobs, Harvey Allen, and associates at NACA evolved theories for explaining the velocity and pressure distribution over airfoils in subsonic flow and means for designing airfoils to have a desired pressure distribution. They also showed that a favorable pressure gradient and a smooth surface could delay the onset of transition from laminar to turbulent flow, thereby materially reducing the drag of smooth airfoils. Following World War II, airfoil design attention was directed mostly to effects of wing sweep, delta wings, and supersonic aerodynamics. Recently there has been increased attention to two-dimensional airfoil theory at high subsonic Mach numbers.

It is now possible to evolve airfoils that have flat top velocity curves at high subsonic Mach numbers. These airfoil shapes are not necessarily the same as those which were evolved to provide a flat top in incompressible flow. This is a step forward in progress.

Another step forward in the progress of airfoil design is the work of Stratford.[19, 20] Stratford suggests that hollow pressure recovery eurves are superior to the linear pressure recoveries designed into the majority of modern airfoils. Although the work of Stratford is not conclusive, even for incompressible flows, it is very valuable because it has opened up the whole subject of defining the optimum flow. The Stratford shapes may be optimum for many cases, particularly in incompressible flow, but a serious question arises whether these flows are optimum when there is a shock at the start of the pressure recovery. Such shocks are inherent in high subsonic Mach number airfoil use. Further research will evolve airfoil shapes for the optimum pressure rise following the shock that is inherently present in all practical aircraft. It is not obvious that leading edges should be shaped to prevent a local high velocity point near the leading edge. It has been suggested by Pearcy[21] that such peaks near the leading edge, followed by constant velocity flow, may be very acceptable.

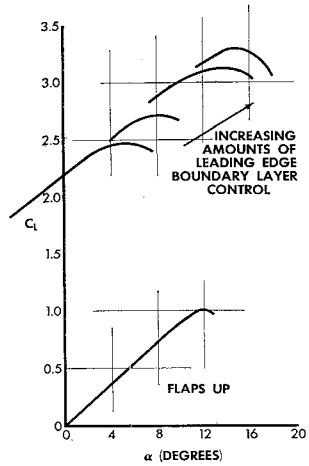

Fig. 6 Possible lift increases with leading edge boundary-layer control.

Another important design tool that is not currently understood is the vortex generator. Appropriately chosen vortex generators might well turn out to be an important part of the optimum solution to the pressure rise problem, particularly if there is a shock involved.

Attention also should be directed toward improving the pressure recovery by boundary-layer control.

With all of the forementioned tools available, it seems timely for a new attack on the problems of high subsonic speed airfoil design. Figure 8 is a diagram of an airfoil designed to have a flat top at high Mach number and using a hollow pressure rise as proposed by Stratford.

Opportunity 7

It appears likely that substantially improved high subsonic Mach number airfoils can be evolved by the application of modern aerodynamic research tools to the problem.

Airfoil Drag Rise

A typical set of drag rise curves for two-dimensional airfoils in the high subsonic Mach number region are shown on Fig. 9. The points on the drag curves indicate where the local Mach numbers attain the values of $M = 1.0$ and 1.2. The attain-

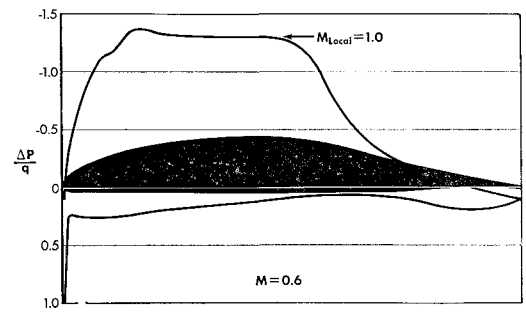

Fig. 8 Pressure distribution characteristics for a typical Stratford section airfoil.

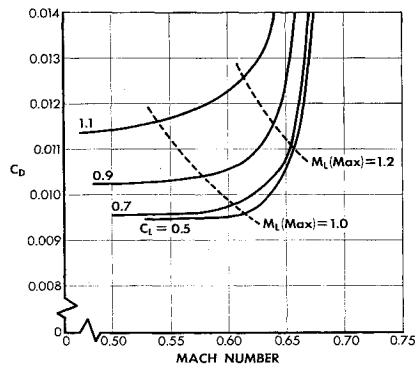

Fig. 9 Variation of C_D with Mach number at constant C_L on a two-dimensional airfoil.

ment of a local velocity of $M = 1.0$ or 1.2 does not appear in itself to be an adequate definition of the point for drag rise. There are probably places on the airfoil where the Mach number can locally exceed $M = 1.0$ without causing much drag rise. The losses incurred in a small shock are not very great and in themselves do not produce much drag rise unless they cause the onset of separated flow and pressure drag.

Opportunity 8

An opportunity exists for the development of a more adequate theory of transonic drag rise on lifting two-dimensional airfoils.

Delayed Drag Rise at High Lift

Figure 10 is a plot to show the Mach number at which drag rise might start for two-dimensional airfoils as a function of lift coefficient and thickness ratio. The lines drawn are suggested as practical working goals for design efforts to attain high critical Mach numbers at high lifts. The data are empirical but are generally based on the attainment of Mach number 1.2 above $C_L = 1.0$ and a local Mach number of 1.0 at $C_L = 0$. Flat top curves are assumed with relatively small regions of pressure recovery. This particular plot is not directed toward the low lift coefficient region where extensive experimentation and development has already occurred, but rather to the region above $C_L = 1.0$ where there has been very little experimentation by aircraft aerodynamicists. Possibly, work has been done in this region by engine airfoil designers.

Opportunity 9

An opportunity exists to develop special airfoils for the high Mach number, high lift coefficient region.

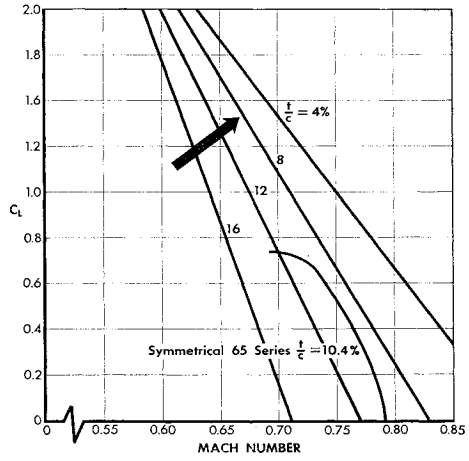

Fig. 10 Goals for drag rise characteristics of two-dimensional airfoils as a function of lift coefficient and thickness chord ratio.

Supersonic Pressure Drag

In his 1946 Wright Brothers' Lecture von Kármán[22] brought attention to the Kármán-Tsien transonic similarity formula. Figure 11 is one form in which this similarity formula has been used for two-dimensional airfoils. This formula is a second-order approximation to the small perturbation theory near $M = 1.0$. In the supersonic region the conventional method of computing drag for thin airfoils fits exactly into the definition used in the Kármán-Tsien formula. This is shown in Fig. 11. It is interesting to note that the Kármán-Tsien formula also applies to three-dimensional bodies such as highly swept wings and deltas, if the lateral dimensions are tied in as well as the thickness dimensions. Kármán covers this in Ref. 23. The conventional theory of supersonic deltas as given by Puckett and Stewart[24] also fits directly into the Kármán-Tsien similarity form if appropriate corrections are made for planform similarity. However, these supersonic delta calculations did not include second- or higher-order perturbation provisions which would materially change the results near $M = 1.0$. An examination of Fig. 11 to determine where drag reductions of two-dimensional airfoils might be possible provides little encouragement in the fully supersonic flow region. Supersonic airfoil theory is simple and generally seems to explain and agree with the facts of the airflow. In the low supersonic region this theory does not work at all, and the requirements of the theory with respect to size of perturbation are not met. Here, the second-order theory developed in Refs. 25–28 gives results in general agreement with the experimental facts.

As covered in an earlier section, there is much room for the development of a more practical theory in the subsonic region. Probably, substantial improvements in the Mach number for a drag rise are possible both by delaying the onset of supersonic flow and also by meeting the special requirements for this region.

The foregoing relates primarily to two-dimensional airfoils. A similar analysis can be made for slender bodies and also for three-dimensional shapes such as deltas and highly swept wings. The conclusions to be drawn for slender bodies are similar to those for two-dimensional wings. The flow over three-dimensional bodies is not well understood near $M = 1.0$. Certainly a tremendous amount of work remains to be done for three-dimensional bodies in delaying the onset of transonic pressure drag.

Opportunity 10

The onset of transonic drag rise can be delayed to a higher subsonic Mach number by attention to the flow processes in this region. A good three-dimensional theory for this region remains to be developed.

Maximum Lift

This section will examine the question of the maximum lift or normal forces that are possible on airfoils at various Mach numbers. For the purpose of this section, lift coefficient will be based on true chord. Circulation theory teaches that if the leading-edge and trailing-edge stagnation points are brought into coincidence, $C_L = 4\pi$. Another possible absolute limitation on maximum lift coefficient can be that of having total head on the lower surface and a perfect vacuum on the upper surface, resulting in $C_{L\max} = H/q$. These limitations on maximum lift coefficient are plotted on Fig. 12. Also plotted on Fig. 12, for reference purposes only, are the four drag rise goals from Fig. 10 and the curves of $M^2C_L = 0.5$ and 1.0. It would be very interesting to see a refined theory of maximum lift vs Mach number. The forementioned limits are only approximate at best. A limiting value of 4π is correct only in incompressible flow; the value may increase somewhat with increasing Mach number. Experimental data and theory show that, once sonic velocities have been exceeded, a bubble exists near the leading edge within which the pressures and

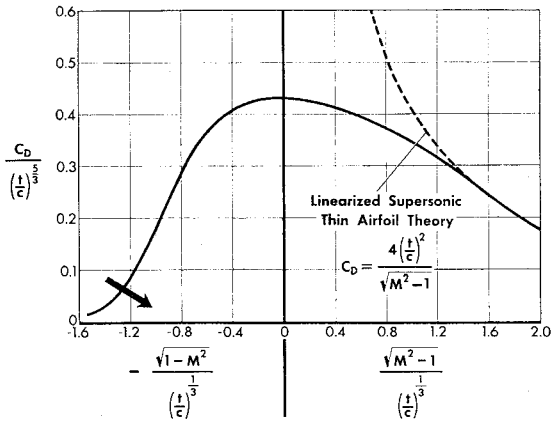

Fig. 11 Drag at zero lift plotted by the Kármán-Tsien transonic similarity law method.

velocities no longer decrease with increasing Mach number. This produces less than a full vacuum on the upper surface and causes the force vector to rotate in a drag direction. Thus the H/q limitation just suggested is more nearly a limitation on maximum normal force coefficient than lift coefficient. This is the so-called lack of "leading edge suction." As the Mach number increases, the supersonic flow region moves further and further aft on the airfoil until at $M = 1.0$ the flow is supersonic over most of the upper surface. Experimental values of upper surface pressure of $0.25H$ have been measured extending from 5% chord to the trailing edge at $M = 0.85$. Above $M = 1.0$ the attainment of negative pressures on the upper surface is less important because of the increased value of H/P_S. In the hypersonic flow region the forces on the airfoil are not greatly changed by assuming an absolute vacuum on the upper surface. Thus, the assumption of vacuum on the upper surface becomes more and more reasonable and attainable with increasing Mach number.

The lower surface presents a different set of problems. At subsonic Mach numbers it is relatively straightforward to obtain high pressures approaching full total head on much of the lower surface. At supersonic Mach numbers, the problem of obtaining high pressures is comparable to that of inlets where pressure recoveries at Mach 3 of $0.85H$ are difficult to attain and the total pressure behind a normal shock is only $0.33H$.

The lines of $M^2C_L = 0.5$ and 1.0 represent the lift coefficients vs Mach number that an airplane would follow in flying at increasing Mach number at constant altitude and constant wing loading. Current practice limits airplane operation to values of M^2C_L below 0.50. $M^2C_L = 0.50$ cuts into the region on Fig. 11 where lift is possible without a drag rise. Not much practical attention has been directed to this problem of maximum lift vs Mach number. High drags are associated with the high angles of attack required in the supersonic region and with the upper surface separation in the subsonic region. Boundary-layer control procedures discussed earlier should make it practical to attain and make practical use of much higher lift coefficients in the subsonic region. The author believes that aeronautical research workers will find much of interest and practical value if they direct attention to the attainment of the highest possible values of normal force vs Mach number.

Opportunity 11

An aerodynamic research attack on the problem of maximum lift and maximum normal force vs Mach number is likely to produce values greatly in excess of anything currently attained experimentally or theoretically understood. In the subsonic flow region the higher lift coefficients are likely to have immediate practical significance for application to aircraft.

Supersonic Swept Wings

In 1935 Busseman[29] introduced the concept of sweepback in supersonic flows. Later, in 1944, Jones[30] introduced the concept of an arrow wing. Based on these two concepts, applied aeronautical research took up the concept of sweepback and made great strides during the 1940's in the development of practical aircraft. Rudimentary theories were developed to explain the flow over these aircraft shapes. The first-order theory says that it is only the Mach number normal to the leading edge that counts in defining the flow processes over the wing. Figure 13 is a plot of the relationship between sweepback, Mach number, and leading-edge normal Mach number. This is a plot of $M_{\text{normal}} = M$ cosine sweep. A modern jetliner flying at $M = 0.85$ with a 35° sweep has a leading-edge normal Mach number of only 0.70. A supersonic transport flying at $M = 2.50$ would require a 74° sweep to attain this same condition.

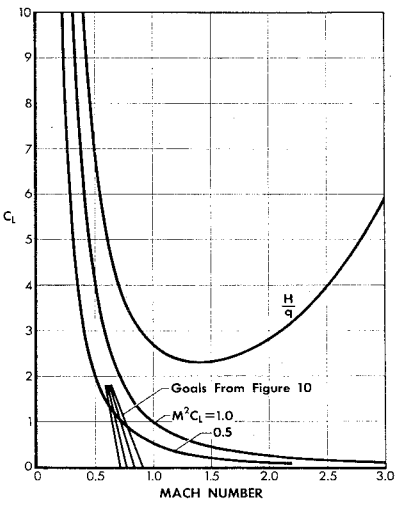

Fig. 12 Absolute limits on maximum lift coefficient as a function of Mach number.

Figure 14 is a plot of P/P_S pressure vs Mach number and shows H, q, and the pressures which correspond to various local Mach numbers in isentropic flow. Shown on Fig. 14 is an airfoil assumed to be operating at zero sweep at $M = 0.7$, 35° sweep at $M = 0.85$, and 74° sweep at $M = 2.50$. Normal leading-edge Mach number is 0.70 for all three cases. The first-order, or simple-sweep theory says that the pressures over the airfoils as a percent of static pressure will be the same under these three conditions. Shown on Fig. 14 are the pressures for a maximum super-velocity local Mach number of 1.0 for the unswept case. At 35° sweep and $M = 0.85$, this results in a local Mach number of 1.11. The maximum local Mach number is 2.70 at $M = 2.50$ and 74° sweep. Since the upper and lower surface pressure diagrams would be identical at each of these three sweep angles, the altitude at which a given

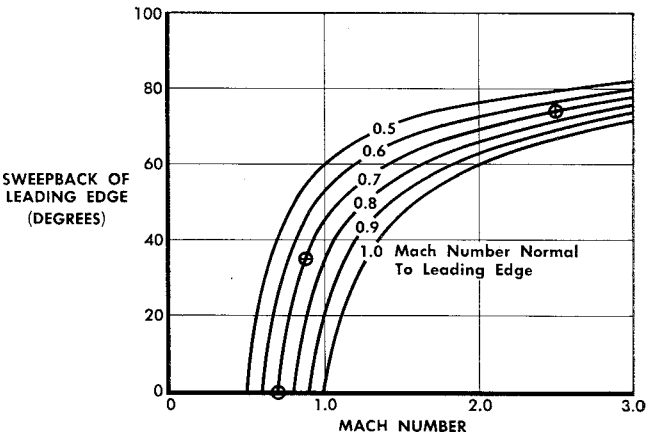

Fig. 13 Relationship between freestream Mach number and Mach number normal to leading edge for various leading edge sweeps.

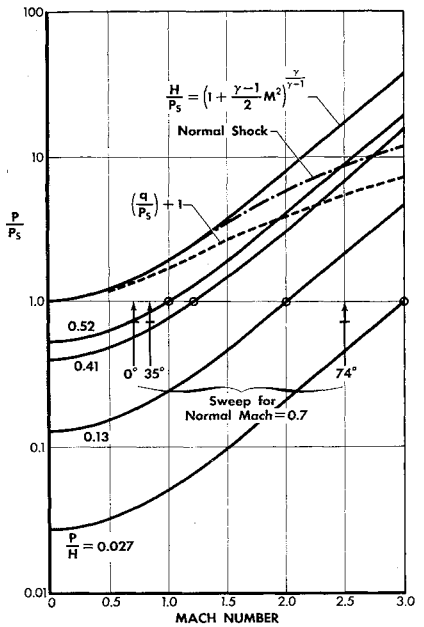

Fig. 14 Pressure ratios at various Mach numbers in isentropic flow.

amount of lift would be obtained at these three Mach numbers and three sweeps would be identical. Under these circumstances no increase in lift at a given altitude is possible at the higher Mach numbers. The lift coefficients corresponding to these three conditions would decrease as the cosine squared of the sweep, and since the Mach number and sweep were chosen to give a constant product of Mach number times cosine, the product M^2C_L is constant.

The practical designer is not likely to limit himself to the altitudes and lift coefficients provided by this simple sweep theory. Many supersonic aircraft will be required to operate at higher lift coefficients than would be provided in the forementioned. The practical designer has incentive to work at attaining the goals suggested on Fig. 10.

The flow over the wing is not straight, and the assumptions inherent in Figs. 13 and 14 cannot be met. The real flow changes direction in the plane of the wing. Sweepback is used for the announced objective of keeping the flow at the leading edge and upper surface consistent with subsonic flow processes. Wings possibly can be developed with leading edges that meet subsonic high lift coefficient flow conditions, while still permitting the attainment of substantial pressure lift on the lower surface further back on the wing. It is not evident that present three-dimensional supersonic wing theory

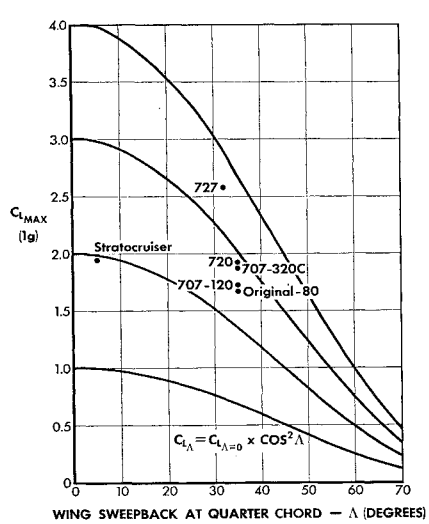

Fig. 15 Effect of sweepback on maximum lift.

makes any provision for applying the boundary conditions necessary to accomplish this. These boundary conditions are not well understood or defined for the subsonic compressible two-dimensional case. The absence of "leading edge suction" on supersonic wings appears to be nearly identical to the two-dimensional subsonic drag rise as on Fig. 9. It is noteworthy that the transonic drag rise below $M = 1.0$ for two-dimensional airfoils is largely the result of increasingly negative pressures on the rear of the airfoil, rather than the result of loss of negative pressures on the leading edge.[25] This implies that the real interest in sweepback is probably in the rear converging portion of three-dimensional shapes where it is desired to get isentropic compression rather than further expansion.

Lock[31] gives some interesting results on swept wings. The author believes that theoretical and experimental research on lifting three-dimensional wings at supersonic Mach numbers will result in a substantially better understanding of the flow processes and some further reduction in drags for the lifting cases.

Opportunity 12

The aerodynamic research engineer has a major challenge to understand, theoretically and experimentally, the flow processes involved over three-dimensional lifting wings at supersonic Mach numbers.

Sweepback and Maximum Lift

The extensive attention given to sweepback over the last 20 years stemmed from the original concept that only the flow normal to the leading edge counted. The introduction of sweepback permitted the development of airplanes that could fly at substantially higher Mach numbers without encountering serious Mach number difficulties. Inherent in the first-order assumption of sweepback effect was the assumption that the lift coefficient at which a particular flow process would occur would be reduced by the cosine squared of the sweep angle. This general concept was applied to the maximum lift coefficient as shown on Fig. 15. Once this plot has been made and the first-order concept of sweep accepted, aeronautical engineers assumed that they had to pay a price in maximum lift coefficient, as shown by the lines on Fig. 15, in order to obtain the sweepback benefits of higher critical Mach numbers. This led to complacency and the acceptance of low maximum lift coefficients in swept-wing aircraft. This simplified theory has delayed the realization that high maximum lift coefficients are actually attainable on sweptback

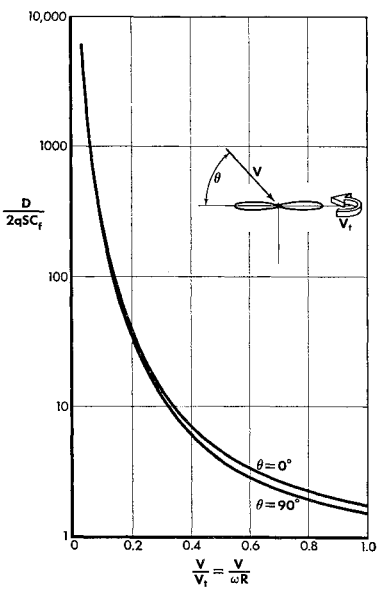

Fig. 16 Drag of a constant chord propeller with zero section lift at all points.

wings. Certainly the pressures on the lower surface of the wing are more nearly a function of the flap sweepback angle than of the leading-edge sweepback angle. There is no obvious reason why the pressures over the upper surface of the flap should be related to leading edge sweep rather than flap sweep. The less positive pressures on the lower surface of flapped swept wings can be explained as a spanwise spillage around the end of the flap. Chordwise flaps might recover the total dynamic head rather than just the dynamic head normal to the leading edge. Figure 15 shows the lift coefficients attained in one g flight on a number of Boeing airplanes. Although the lift coefficients are based on the wing area with the flaps and slats retracted, the author believes they show quite clearly that the sweepback limitation on maximum lift coefficient is not a real one.

Opportunity 13

High maximum lift coefficient will be attained on swept wings.

Propeller and Rotor Drag

A hypothetical propeller can be carried through the air and powered by a motor in such a way that each section of the propeller is operating at zero lift with respect to relative wind and, thus, is providing only drag. The power put into the shaft to turn this propeller can be converted to drag by dividing by forward velocity. It is assumed that all sections are at zero lift simultaneously, which is hardly ever realized on real propellers. The drag of such a propeller with constant chord blades is shown on Fig. 16 as a function of V/V_t, the ratio of forward speed to rotational tip speed. (Note that this is not exactly the same as the μ used by helicopter engineers.) The drag is plotted as a multiple of that which the same propeller blades would have if feathered and untwisted. It is evident that the drag of a propeller when producing no thrust will run from 1–10 times the feathered and untwisted drag.

A similar calculation can be made for a helicopter rotor or propeller operating with the air at right angles to the shaft. In this case the propeller or rotor is assumed to have no twist and no pitch. The losses in this case are about 10% higher than when the shaft is directed into the wing. This friction drag can be a large part of the drag of aircraft with large propellers, such as tilt-wing aircraft. It is a large part of the drag problem of helicopters at high speed. It is evident that this drag can be reduced very materially by reducing the rate of rotation of the rotor or propeller. Only a small reduction results from changing the inclination into the airstream.

Opportunity 14

Large reductions in propeller and rotor drag may be possible by reducing their rotational velocity.

Rotor Compressibility Losses

It is very unreal to neglect compressibility losses in considering the drag losses on a rotor. All propellers and rotors are designed with compressibility in mind and invariably operate at design conditions with substantial compressibility losses. Propellers have always been built with the lowest practical structural thickness ratio near the tip. Helicopter rotors, on the other hand, have conventionally used 12% or thicker tip sections; the choice was based primarily on the maximum lift characteristics of the sections. Airfoil developments for lift and for compressibility improvement, as described in other sections of this paper, should permit the choice of airfoil sections for helicopter rotors that give materially improved compressibility performance.

Opportunity 15

Better airfoil sections can be developed to provide lower compressibility losses in helicopter rotors.

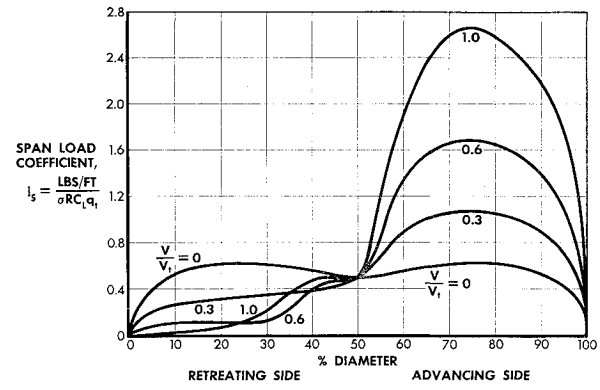

Fig. 17 Spanwise lift distribution on a lifting rotor with all elements working at fixed lift coefficient.

Rotor Lift

When a helicopter rotor or propeller goes through the air with the shaft at right angles to the airstream, the dynamic pressure is increased on the advancing blade and materially reduced on the retreating blade. A hypothetical rotor can be described on which all elements of the airfoil operate at all times at a fixed-lift coefficient. This is done by means of blade twist and pitch, with the twist and pitch being made a function of the azimuth and operating conditions. Under such circumstances the maximum lift which can be carried at any part of the rotor is a function of the advance ratio V/V_t and of the assumed lift coefficient. Figure 17 presents the spanwise distribution of lift which is encountered on such a rotor. There is a large reduction in lift on the retreating side and large increases in lift on the advancing side. The net result is large rolling moment, since most of the lift is carried on the advancing side.

Practical rotors will attain lift along their diameter as shown on Fig. 18 for the assumed case of $V/V_t = 0.45$. An ordinary articulated rotor operates with the moment of the lift on the blade constant with azimuth angle. The advancing blade operates with some download at the tip and considerable upload on the inner portion. The lift at the center of the rotor diameter is contributed mostly by the fore and aft direction blades; it is less on articulated rotors than is possible on a maximum lift rotor, in order that the lift moments about the articulation hinge will be the same as for the retreating blade, which has the limiting lift moment.

The application of a second harmonic pitch angle variation with azimuth makes it possible to load the fore and aft blades to lift moments that are greater than the lift moment on the retreating blade. It is possible to increase the lift on the advancing blade by the use of flaps or high twists. This produces a large shear load at the hub which materially assists the lift of such a rotor while still keeping the lift moment of the advancing blade equal to that of the retreating blade. This requires a greater download on the advancing tip. Such a rotor with cyclic pitch change and with additional lift on the

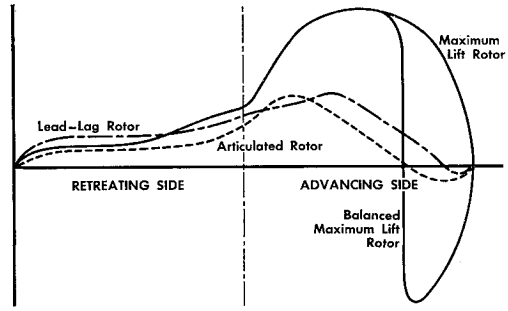

Fig. 18 Spanwise lift distribution on different types of rotors.

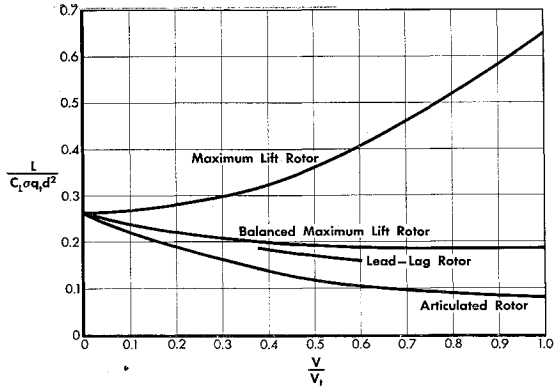

Fig. 19 The effect of forward speed on rotor lift at constant rotational speed in terms of tip dynamic pressure.

advancing blade is shown on Fig. 18 and is labeled "Balanced Maximum Lift Rotor."

Derschmidt[32] has proposed a lead-lag rotor in which the velocity of the retreating blade is increased and the velocity of the advancing blade is decreased to provide nearly constant tip velocity with azimuth. This increases the lift available on the retreating side and thereby permits still more lift on the advancing side. The skin friction drag of Fig. 16 is also reduced on lead-lag rotors.

The lifting ability of these four types of rotors is shown on Fig. 19. Figure 19 is a plot of the variation in the maximum lift that a rotor can carry as influenced by the maximum section lift coefficient and forward speed at constant rotational speed. It is evident that the lift which a helicopter rotor can carry is materially reduced with increasing forward speed. The ceiling of a helicopter as limited by the stalled lifting ability of the rotor will be a maximum in the hover case. This assumes that adequate power is available. In many helicopters high speed is limited, not by drag but by the stall of the rotor, as indicated on Fig. 19.

Figure 20 is a replot of the same data from Fig. 19 except that the data are presented in terms of freestream q rather than rotor tip q. This further emphasizes the loss in lifting ability of a rotor as compared to an ordinary wing.

Opportunity 16

There is both a requirement and opportunity to increase the lifting capability of rotors at high forward speeds.

Rotor Induced Drag

Figure 21 is a plot of the effective span-to-diameter ratio vs advance ratio V/V_t for the four different rotors described in the previous paragraphs. These data were calculated from span lift distributions, such as those on Fig. 18, by the Fourier

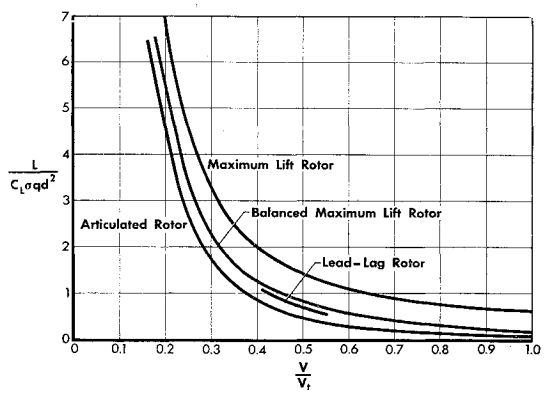

Fig. 20 The effect of forward speed on rotor lift at constant rotational speed in terms of freestream dynamic pressure.

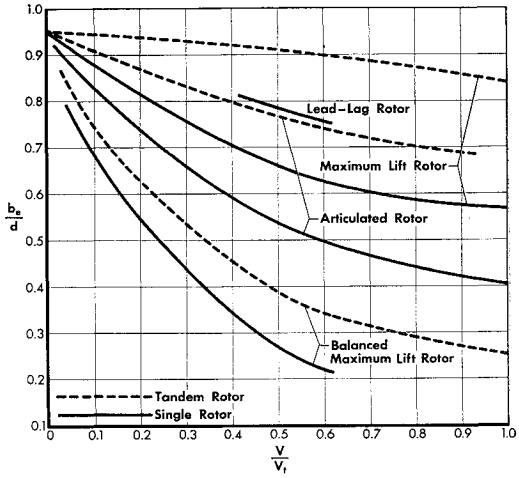

Fig. 21 Effective span of rotors for different advance ratios.

series method.[33] The objective in making this calculation was to come to a better second-order approximation of rotor-induced drag than comes about from the first-order approximation of constant inflow which is ordinarily used and which represents a value of the effective span-to-diameter of 1.0. The induced drag is increased by the inverse square of the effective span-to-diameter ratio. Possible increases in induced drag greater than 100% are indicated on Fig. 21. Rotor aerodynamics specialists point out that this second-order calculation is very inadequate and almost certainly underestimates the induced drag for most cases. It is presented here to indicate that a better value than constant inflow is available and in the hope that the work of Miller[34] and others can be extended to provide more exact definitions of real induced losses in a rotor.

The rotor-induced drags shown here do not necessarily apply to complete helicopters. If the helicopter has two rotors turning in opposite directions, the two load distributions must be added before computing the induced drag. More nearly elliptical span loading will be obtained as shown on Fig. 21. The values on Fig. 21 are for both single- and tandem-rotor helicopters. Tandem rotors, when flown with yaw, can probably have effective spans greater than rotor diameter.

Opportunity 17

Recent advances in helicopter rotor calculation methods can be extended to give a much more adequate definition of the induced losses in a rotor.

Rotor Performance

Helicopter rotor performance can be presented conveniently in a lift vs drag presentation similar to that used by the fixed-wing designer. One possible way of doing this is to plot L/qd^2 vs D/qd^2 as shown on Fig. 22.

This terminology is identical with C_L/A and C_D/A. Shown on Fig. 22 are lines of induced drag as constant effective span-over-diameter. The effective spans for various lifts can be taken from Fig. 21 and other such data.

The zero lift drag of an untwisted rotor is described on Fig. 16 and can be plotted directly along the abscissa of Fig. 22 as a function of V/V_t and rotor blade area factor σ = blade area/disk area. The plotted data on Fig. 22 are for $\sigma = 0.10$. The maximum lift that can be obtained from a rotor can be taken from data such as that in Figs. 19 and 20. The values from the ordinate of Fig. 20 are multiplied by σ to obtain the lifts for Fig. 22.

Assuming no compressibility losses and no variation in profile losses with section lift coefficient, lines of rotor drag vs lift can be drawn for each value of V/V_t by preceeding from the

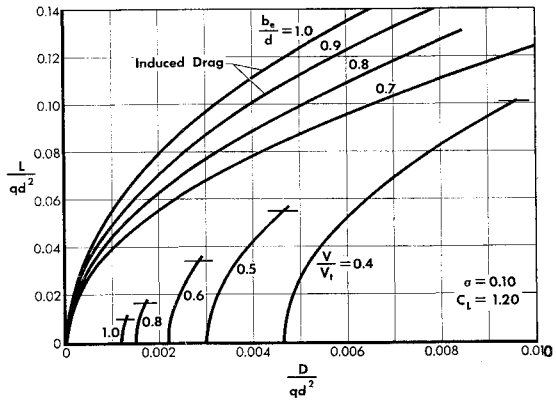

Fig. 22 Rotor lift drag polar.

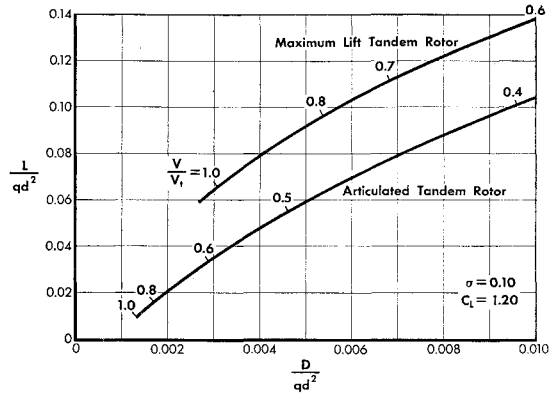

Fig. 23 Comparison of polars for different rotor types in incompressible flow.

drag at zero lift parallel to the effective span lines up to the maximum lift cutoffs as shown on Fig. 22. These drags must then be increased for the increase in profile loss with lift coefficient and also for compressibility losses. For simplicity of presentation, neither loss has been shown on Fig. 22.

Figure 22 is suggested as a practical means for presenting rotor data, whether computed by exact methods or by approximate methods. It is a convenient way to understand the different losses and compare different rotor systems. It is noteworthy on Fig. 22 that to reduce the profile losses high values of V/V_t are desired, but for articulated rotors these high values of V/V_t produce very large losses in available lift. If the lift could be held high while slowing down the rotation of the rotor, very much improved lift-drag ratios could be obtained.

Opportunity 18

Methods can be devised for calculating and presenting helicopter rotor performance that will clarify rotor limitations toward the end of more rapid progress in rotor development.

Alternate Rotor Designs

On Fig. 23, two of the rotor types described in previous paragraphs are compared for the incompressible flow case. These are envelopes of the data for different advance ratios V/V_t.

When applied to helicopters, the simple calculations implied in this paper are not always completely applicable, since it may be desirable to compound the helicopter by using a wing, and because there is some variation in the performance presented with tilt of the rotor, as required to provide thrust. Both of these considerations are readily added to the methods of presentation used in this paper.

Opportunity 19

Large opportunities exist for the improvement of helicopter rotor performance.

Theory of Low-Speed Powered Flight

Theories of low-speed powered flight have been developed by helicopter engineers, but only recently has there been much attention to this problem by fixed-wing engineers. The new interest comes from the development of direct jet-lift aircraft, tilt-wings, tilt-propellers, and other such aircraft. The construction shown on Fig. 24 provides a first-order approximation to a theory of low-speed powered flight. Induced drag, as expressed in the first-order theory of Prandtl,[35] $C_{D_i} = C_L^2/\pi A$, and as refined by Helmbold[5] and others, is invariant when plotted $L/qd^2 = C_L/A$ vs $D/qd^2 = C_D/A$. Figure 24 is plotted in these terms. The theoretical induced drag for unpowered gliding flight is shown. Also shown is a typical polar of a highly flapped airplane. If it is assumed that there is no interaction between the lifting system of the wing and the air flowing either into or out of the powerplant, then a construction is possible which plots the inlet drag as a vector parallel to the drag direction and of quantity equal to the mass flow of air passing through the propulsion system times the free-flight velocity. This is shown for three different lifts of the representative aircraft on Fig. 24. If it is assumed that a thrust deflection device is available, which permits deflecting the gross thrust of the air leaving the power plant, then the further construction of gross thrust power vectors shown on Fig. 24 is possible. The envelope of the resultant airplane-plus-inlet drag-plus-deflected gross thrust is a first-order approximation to the lift-drag relationships possible from the combination of powerplant and airplane. It assumes no interactions between wing, inlet air, and deflected jet.

Using this construction, three different lift-drag-power relationships are constructed (Fig. 25, taken from Ref. 36). The data labeled "Wing Plus Jet" on Fig. 25 are the theoretical Helmbold induced drags (Fig. 24) plus a noninterfering deflected jet thrust at such a high velocity that zero inlet drag could be assumed. The data labeled "Turning Vane" on Fig. 25 are the lift-power-drag relationships which would be obtained for the hypothetical case of an ordinary propeller always directed into the direction of flight, with a set of turning vanes behind it deflecting the gross thrust of the propeller. In this "turning vane" assumption, no interference is assumed between the deflected propeller slipstream and the air entering the propeller. No wing lift is assumed in this case, except for the turning vane effect on the air which went through the propeller. In both the "turning vane" and "wing plus jet" cases, the deflection of the gross thrust is assumed to be in the optimum or envelope direction.

The third case presented on Fig. 25 is the "Spherical" case used by some helicopter engineers and as suggested by Haffner.[37] In this case the quantity of air reacted upon is that which passes through a sphere equal to the diameter of the

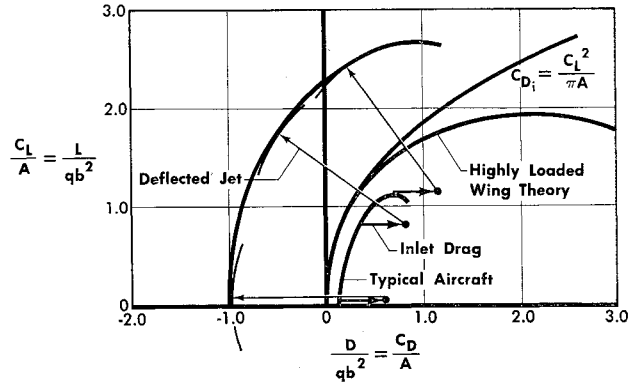

Fig. 24 Vector diagram for wing-deflected jet combination.

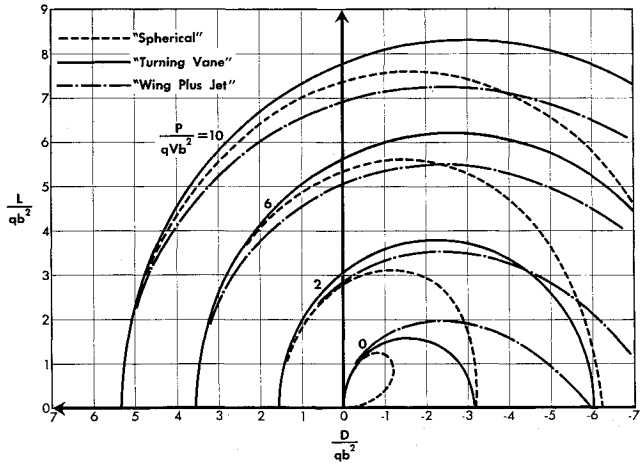

Fig. 25 Comparison of force polars.

rotor, but interaction is assumed between the gross deflected thrust and the inlet air. The quantity of inlet air is assumed to be materially reduced by the gross thrust when a component of the deflected thrust is directed contrary to flight direction. Here, again, no direct wing lift is assumed, but this and the other two theories give nearly identical induced drags in the region below $L/qd^2 = 1.0$. This is where nearly all flight operations of unpowered flight occur.

A deflected-slipstream airplane or a tilt-wing airplane might well have still better lift-drag relationships than those suggested by the construction on Fig. 25.

Opportunity 20

An opportunity exists for the development of a rigorous theory of low-speed powered flight.

Deflected Thrust

The low-speed thrust vs speed requirements of a deflected-jet thrust airplane are shown on Fig. 26. These calculations are based on a high-speed noninteracting jet in which the gross thrust is equal to the net thrust—the "wing plus jet" case on Fig. 25. Data are presented for two different deflection angles. In the first case there is no deflection and the jet thrust is parallel to the direction of flight. In the other case the jet thrust is deflected in the direction which gives minimum thrust requirements for flight. Figure 26 also shows the effect on thrust requirements of limiting the maximum lift available from the wing to three different values of $C_{L\max}/A$. With no jet deflection, the maximum lift coefficient is extremely important in defining the minimum flight speed; very large thrusts are required parallel to the flight directions as the speed is slowed down to the point where eventually the lift-drag ratio of the wing is equal to 1.0. At this point, the thrust requirement is the same as would be required to fly at zero speed if the thrust had been deflected. The importance of obtaining high lift coefficients when combined with optimum deflection of the jet thrust is materially reduced, but it is still well worthwhile striving for values of C_L/A approaching 1.0.

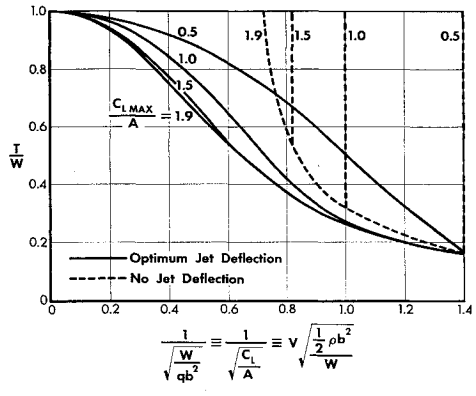

Fig. 26 Thrust required at various forward speeds with undeflected and optimum deflected jets.

It is evident from Fig. 25 that large air-consuming powerplants, such as propellers or rotors, will give some further reduction in thrust requirements vs speed. Furthermore, there is a substantial difference between level flight, climbing flight, and descending flight. The data presented on Fig. 26 are for level flight.

Figure 27 is a further explanation of the deflected-slipstream case. The aerodynamic lift and the aerodynamic drag of the basic airplane add to give the basic aerodynamic force vector on the airplane. Added to this is the inlet drag for the amount of air that is slowed from flight velocity to zero velocity as it enters the airplane system. This inlet drag assumption works perfectly well for propellers. The weight of the airplane is shown as a vector directed toward the ground. All other vectors are parallel or perpendicular to the flight direction. The gross jet thrust must be deflected to such an angle as to close the vector diagram. It is only that component of the gross jet thrust directed toward the ground which opposes the gravity force, and which can reduce the aerodynamic lift and drag requirements on the airplane, so as to allow lower forward speeds in flight. For the average descent case, the inlet drag is relatively small and the gross jet thrust must be directed generally toward the ground. Thus, to a first approximation, deflected thrust schemes will give very disappointing performance unless the deflection angles provide for direction of the gross thrust into the vertical direction, with the airplane flying along the desired descent path.

Opportunity 21

Deflected thrust schemes that direct the powerplant thrust in a vertical direction will provide reductions in minimum flight speeds.

Jet Flaps

The work of Spence,[38, 39] and as extended by Yoler,[40] and Maskell and Spence,[41] shows that jet flaps will provide very large increments of lift. The jet flap is a special case of powered flight. The question then arises: "How does it compare with other powered flight schemes?" The work of Reid[7] and associates at Stanford, and the theory of jet flap drag[42] suggest that nearly all of the jet flap jet momentum is recovered as a forward thrust. This is consistent with the "wing plus jet" construction of Fig. 25 and assumes that the jet is deflected in the optimum direction. A question arises concerning the actual effective angle of the deflected jet of a jet flap. The theory suggests that insofar as drag is concerned, this angle is parallel to the jet sheet direction at a long distance downstream. This assumes no mixing of the

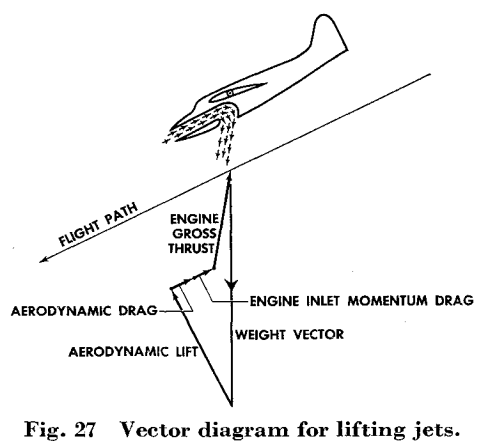

Fig. 27 Vector diagram for lifting jets.

jet as it turns the corner and that the jet then goes nearly parallel to the flight direction.

Figure 28 is a diagrammatic representation of the question of the difference between a jet flap system and a wing-plus-deflected jet system. In the deflected jet case, it is assumed that the wing lift is maintained at potential flow values by the use of boundary-layer control and that the momentum added by the boundary-layer control is equal to the friction drag. Thus, no propulsion or thrust results from the boundary-layer control. These questions then arise: "Are these two cases equivalent?"; "What are the equivalent jet deflection angles of the two cases?"; "What is the thrust vs speed requirement for the two cases?" As a first approximation it would appear that the thrust vs speed requirements are identical. A serious question remains concerning the deflection angle for the jet flap case and the requirements to permit powered flight in descent with jet flaps.

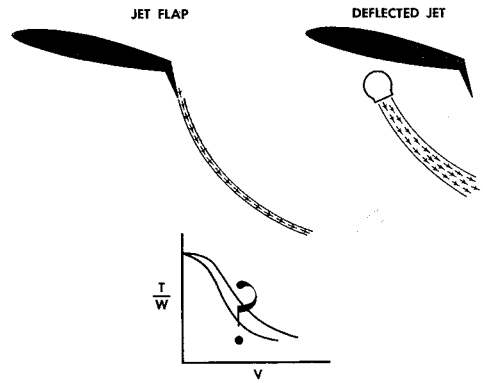

Fig. 28 Jet flap vs deflected jet.

Opportunity 22

Fundamental experiments and theory extensions are required to explain and compare adequately the jet flap airplane case with other powered lift systems.

Deflected Slipstreams

Much attention is currently being directed toward deflected propeller slipstream systems, including aircraft like the Ryan Model 92, the Vertol V-76, the XC-142, the Breguet 941, and Canadair Model CL-84. In these schemes the propeller accomplishes a portion of the slipstream turning or deflection by forces mostly along the shaft and relatively small forces at right angles to the shaft. The remaining deflection of the slipstream is accomplished by the wing which operates in the slipstream of the propeller. Wing-propeller interactions were never thoroughly studied or understood throughout the era of propellered aircraft. Flight and wind-tunnel data always showed large reductions in minimum flight speed when operating with large amounts of propeller power. The popular explanation was that the slipstream by its turbulence—or possibly as a function of the increased velocity going past the wing, or some mysterious characteristic—delayed the stall of the wing and caused the wing lift to increase in a manner comparable to that provided by a slat. A fairly adequate theory of wing lift in the slipstream was developed by Smelt and Davies[43] but is inadequate for large deflections and was never extended to explain the measured performance of the many propellered aircraft for which wind-tunnel and flight data exist.

Figure 29 presents some test data and the double prime method of looking at the deflected propeller slipstream case. This evolved in the course of looking at deflected slipstream airplanes in which all of the wing is in the slipstream. The data on the right on Fig. 29 are the conventional $C_L - C_D - T_C''$ relationships for a propeller and unflapped wing operating together. On the left side of Fig. 29, the double-prime wing lifting performance is presented with wing lift expressed in terms of the dynamic pressure it experiences in the slipstream, and with the angle of attack of the wing corrected for deflection by the propeller. No deflections as the result of forces normal to the shaft were assumed. The wing lifts and the wing stalling angles are adequately explained by this construction. The breaks in the lift vs drag curves for the total configuration seen on the right of Fig. 29 are explained in terms of wing stalling. By definition, operation at $C_D = 0$ is level flight. Level flight would not be possible at the high lift coefficients of Fig. 29 without operating in the stalled region. Descent is still further in the stalled region, and a substantial angle of climb would be required to reduce the wing angle below the stalling region.

By the use of wing flaps and slats, the relationship between the wing and the propeller can be modified to the extent that operation is possible in level flight without wing stalling. Great difficulties are being encountered in the search for schemes that will allow sufficient deflection of the propeller slipstream to permit reasonable angles of descent, without having the wing exceed its stalling angle. Most of the workable schemes result in speed vs power relationships that are far above the optimum which might be expected from the construction of Fig. 25. It is not evident that this problem of powered descent has been adequately solved in helicopters which frequently have high vibrations and high power requirements in high rates of low-speed powered descent. The Vertol V-76, as described in Ref. 44, and the Breguet 941, as described in Ref. 45, show the great progress which has been made in recent years in understanding this problem of powered descent of deflected slipstream airplanes. In both cases much opportunity appears for material reduction in the powers required to attain low-speed flight.

Opportunity 23

A better theoretical and experimental understanding of the interaction between propeller slipstreams and wings is likely to result in marked improvements in performance and handling characteristics of deflected slipstream airplanes.

Ground Effects

The foregoing discussion of powered low-speed flight neglects ground effect. Theoretically and experimentally, ground effect reduces the drag of wings operating near the ground and reduces the power required to produce a given amount of lift from a propeller or rotor. Thus, if there were no adverse interactions between slipstreams and wings the thrust requirements should reduce in the presence of the ground, as shown by the lower lines on Fig. 30. Many experiments have shown that in the presence of the ground the slipstream can interact with the wing, body, and other parts of the aircraft to produce a download on these components.

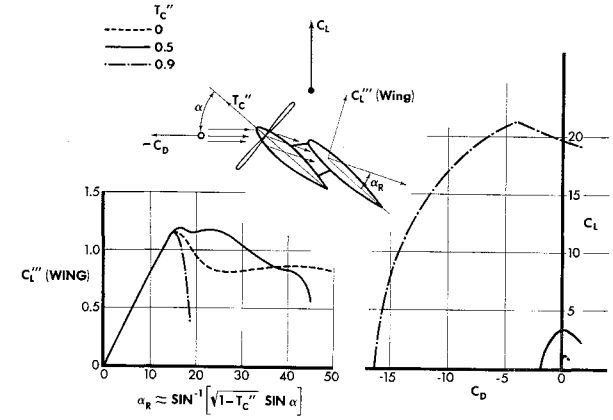

Fig. 29 Lift-drag characteristics for propeller-wing combination based on slipstream and remote dynamic pressure.

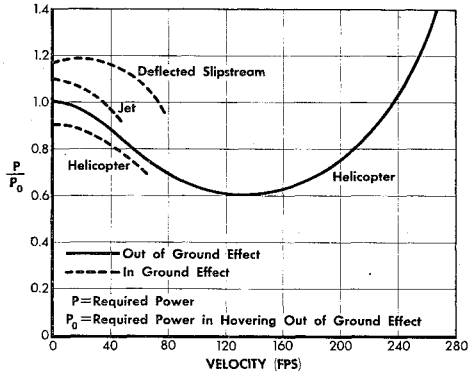

Fig. 30 Ground effect on thrust requirements of some V/STOL systems.

The net result is that the typical jet-lift aircraft requires more thrust to fly in the presence of the ground than it requires in free flight. This is shown on Fig. 30. Theory and experiment have shown that some arrangements with tilted propellers are particularly subject to adverse ground effects (probably stalling), as shown on Fig. 30.

Opportunity 24

Powered-lift aircraft can and should be developed to have favorable ground effect.

Short Takeoff and Landing

With the principal exception of the Breguet 941, low-speed powered flight experiments have been directed largely toward flying at zero speed in the VTOL mode. Other low-speed flight modes have been considered as transition conditions. VTOL requires that the thrust equal the weight. There is a very important region intermediate between the normal airplane region and the VTOL region, which is commonly called the STOL (short takeoff and landing) region. In this region the thrust is less than the weight, but proper use of the thrust may permit flight at much lower speeds than would otherwise be possible. Figure 31 is a diagrammatic representation of this region to show that attention to the VTOL mode does not in any way automatically carry with it attention to the STOL mode. Proper choice of deflection systems, wing flaps, etc., can provide very material reductions in the minimum speed and, hence, in takeoff and landing distance, without requiring that the thrust approach the weight of the aircraft.

Opportunity 25

Attention to the STOL mode, where the thrust is less than the weight, will provide large improvements in minimum flight speed and takeoff and landing distances.

Propeller Performance

In recent years the propeller has largely gone out of use and most propeller research has stopped. The performance characteristics of a typical propeller, 0.13–0.05 thickness ratio[46] are shown on Fig. 32. For the range of thrust loadings given on Fig. 32, propeller losses due to induced effects do not exceed 2%. It is evident that any increase in the thrust carried by the propeller results in an earlier onset of compressibility effects. Operating the propeller at low loadings permits operation to higher Mach numbers. Also shown on Fig. 32 is the envelope performance available from a thinner (0.06–0.02) propeller.[47]

Figure 33 is the same data as Fig. 32, except that all the propeller efficiency losses of Fig. 32 are presented as power losses. Power loss is the power put into the propeller that does not result in a forward thrust. This power is measured in terms of forward flight q and the area of the propeller blades. It is evident that the propeller as a whole behaves

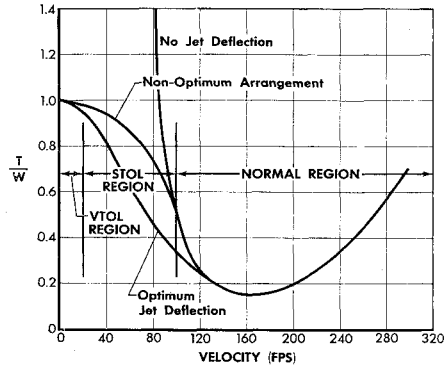

Fig. 31 Thrust requirements of short takeoff and landing (STOL) aircraft for different lifting system designs.

very nearly the same as a two-dimensional airfoil. It has drag and compressibility effects, with an increasing lift very similar to those of an airfoil. The data on Figs. 32 and 33 are envelope values at optimum-blade angle. The propeller pitch was generally in the vicinity of 55°. The propeller was operating at a forward-to-tip speed ratio of about 1.0. Figure 16 shows that the drag would be 1.6 times as great as if the propeller had been feathered. This seems consistent with the drag values shown on Fig. 33.

Opportunity 26

Propellers have very high efficiencies below $M = 0.7$. The high-speed characteristics of propellers can be simply explained in terms of power or drag losses based on blade area, advance ratio, loading, and Mach number.

Ducted Fan Propulsion

Most modern aircraft are powered by turbofan powerplants in which a substantial percentage of the propulsion comes from air that has been acted upon only by the fan portion of the powerplant. This section relates to the propulsive efficiency of this air which goes through the fan; it does not relate to the air going through the gas generator which, in turn, drives a turbine that drives the fan. This engine air also provides propulsion by its residual velocity. The propulsion which can be provided by a fan driven by shaft horsepower is shown on Fig. 34 for various fan pressure ratios at a forward Mach number of $M = 0.40$. The top line on Fig. 34 shows the propulsive efficiency that is possible from a ducted fan installa-

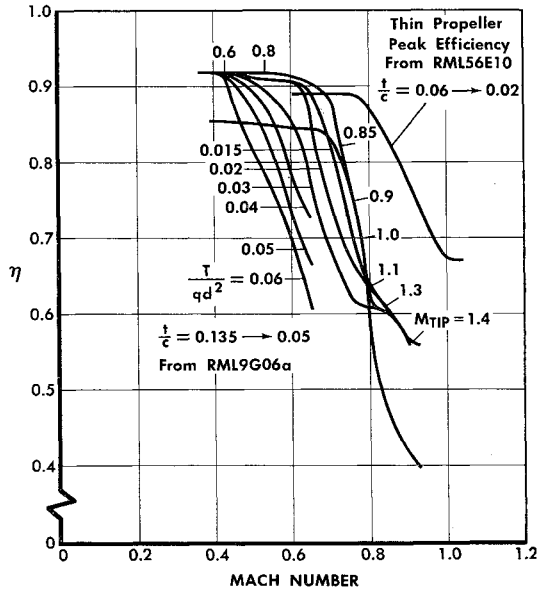

Fig. 32 Performance characteristics of propellers with two different thickness ratios.

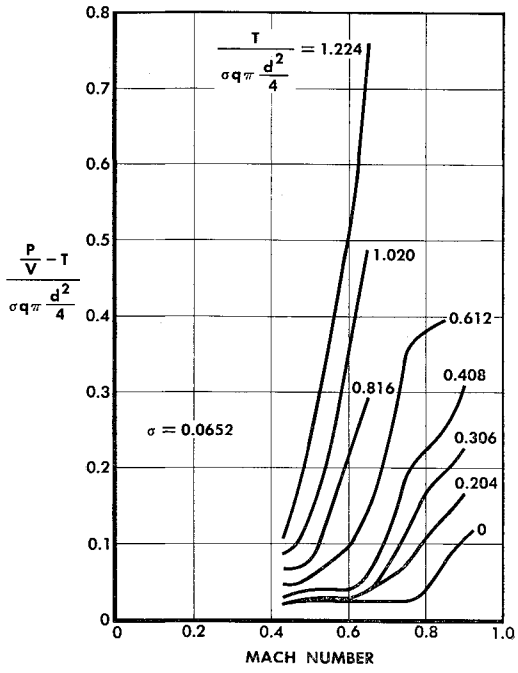

Fig. 33 Propeller power losses.

tion with no internal or external losses and a 100% efficiency. The propulsive efficiency losses are inherent in the high-velocity exhaust. This is identical to the Glauert or Froude definition of propulsive efficiency. On Fig. 34 the efficiencies have been reduced to provide for real fan efficiencies of about 90%. The next increment of efficiency reduction on Fig. 34 assumes a jet nozzle velocity coefficient of 0.98 rather than 1.00. This provides for the internal losses of the air flowing to the compressor, and from the compressor out the fan exit and over the outside of the body. The last increment shown is the external drag of the shroud around the fan. Typical values of the fan shroud length-to-diameter ratio are 1.0 at a fan pressure ratio of 1.0, varying to 1.5 at a fan pressure ratio of 2.0, and a length-to-diameter ratio of 3.0 at a fan pressure ratio of 2.0, and a length-to-diameter ratio of 3.0 at a fan pressure ratio of 14. A wetted area drag coefficient of C_f = 0.003 was used. Propulsive thrusts per pound of air per second

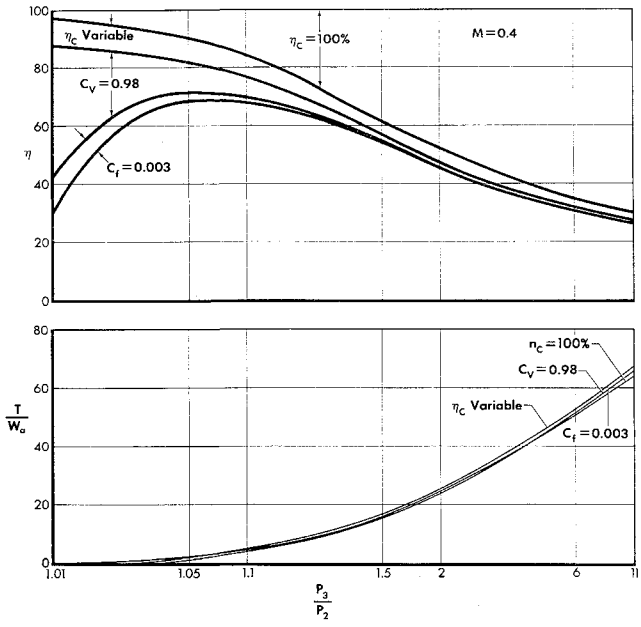

Fig. 34 Fan propulsion characteristics at various pressure ratios for M = 0.4.

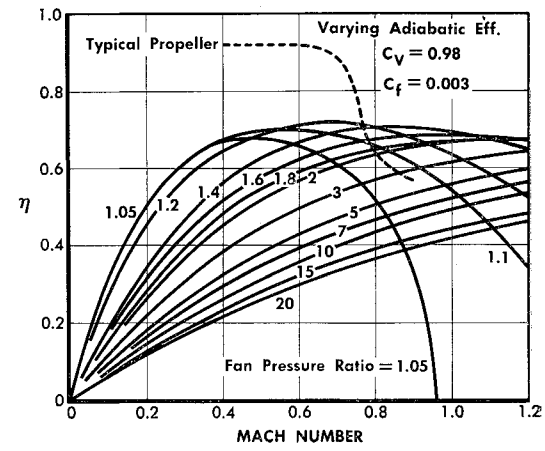

Fig. 35 Propulsive efficiency of ducted fans.

are shown on the lower part of Fig. 34. Data such as that from Fig. 34 are cross-plotted on Fig. 35 as lines of efficiency vs Mach number at different pressure ratios. Also plotted on Fig. 35 are the propeller efficiencies from Fig. 32. It is evident that propellers are substantially more efficient than ducted fans at Mach numbers below 0.6. It is also evident that a propeller is not competitive at the M = 0.8 cruising speeds of modern jet transports.

The shroud over a ducted propeller does not ordinarily reduce the Mach numbers to which the propeller will be subjected. In addition, the shroud drag must be subtracted from the propeller performance. Shrouded propellers have pressure ratios of less than 1.05 and will show efficiency characteristics consistent with an extrapolation below the 1.05 line on Fig. 35. Even if a portion of the shroud or duct were credited as lifting surface, ducted propeller arrangements will leave much to be desired at high forward flight speeds.

Opportunity 27

At low-flight Mach numbers the unshrouded propeller continues to offer efficiencies unavailable by any other means. Ducted fans have superior efficiency at high-flight Mach numbers.

Off-Design Fan Performance

The data on Fig. 35 show that ducted fans with 1.3 pressure ratio have excellent propulsive characteristics at high Mach numbers. At low Mach numbers lower pressure ratio fans and propellers are more efficient. Figure 36 shows the fan performance grid for a typical 1.3 pressure ratio fan. Such a fan would give optimum propulsive efficiency at M = 0.8. When used in an actual airplane, such a fan could not operate at its design point under all circumstances. Aircraft thrust requirements vary with Mach number, altitude, and other circumstances of flight. It would only be happenstance if the fan from Fig. 36 could operate continuously at its design point. To provide less than rated thrust, the fan would be operated at reduced rpm. Under some circumstances the fan

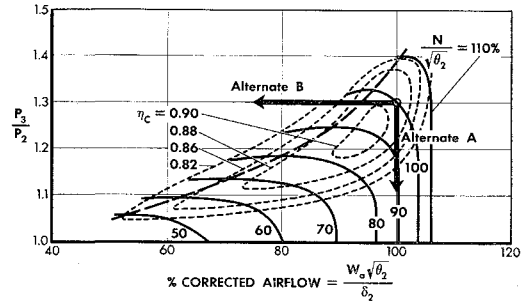

Fig. 36 Fan performance grid (pressure ratio 1.3).

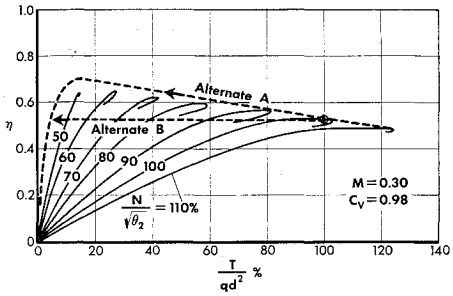

Fig. 37 Ducted fan efficiency at off-design conditions for $M = 0.3$.

duct exit area might be changed to have the fan operate under more nearly optimum circumstances. In any case, the fan must be operated well away from its stall region and away from the unrestricted high-flow condition where power losses are high and propulsion is small. A comparison is made on Fig. 37 of the propulsive efficiency of the fan of Fig. 36 at various thrusts and at $M = 0.3$.

Also shown on Fig. 36 is the performance of a hypothetical alternate fan A, which has only 100% airflow and reduces thrust by reducing pressure ratio. Its efficiency is assumed to be constant as the pressure ratio is reduced. Also shown is alternate B, where the pressure ratio is held constant and the airflow is reduced, to reduce the propulsive thrust.

The propulsive efficiencies of these three cases are shown on Fig. 37. Reduced thrust operation of the fan results in increasing efficiency. The flat top efficiency curves infer that little or no change in exit area would be required to keep the fan operating at its optimum conditions. The external drag of the fan installation is not included in these propulsive efficiencies. Alternate fan B (constant pressure ratio and reducing airflow at constant fan efficiency) has a propulsive efficiency of 53% as shown on Fig. 37. Alternate fan A shows that maintaining a higher airflow than is possible, while staying on the fan characteristics, will give somewhat higher efficiencies at reduced thrust. As zero thrust is approached the high internal losses that go with high airflow sharply reduce the propulsive efficiency of alternate A.

Opportunity 28

Off-design fan performance at low Mach numbers can be improved.

Simple-Cycle Gas Turbines

The simple-cycle gas turbine as a source of shaft power is yet to come into its own. Figure 38 is a plot of the specific fuel consumption vs specific power possible from typical simple-cycle gas turbines at sea level. They are presented as functions of compressor pressure ratio and turbine inlet gas temperature for typical compressor and turbine efficiencies. It is evident that tremendous improvements in specific power are possible from operation at higher temperatures. The optimum compressor pressure ratio goes up with increasing temperature and the net results is a major improvement in

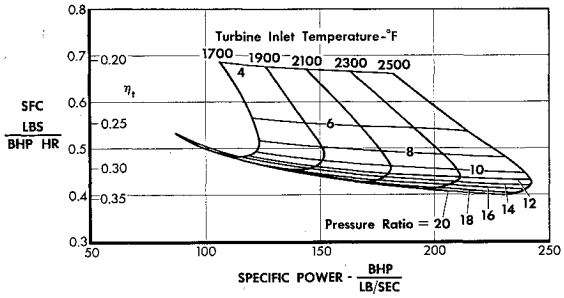

Fig. 38 Simple-cycle gas turbine performance.

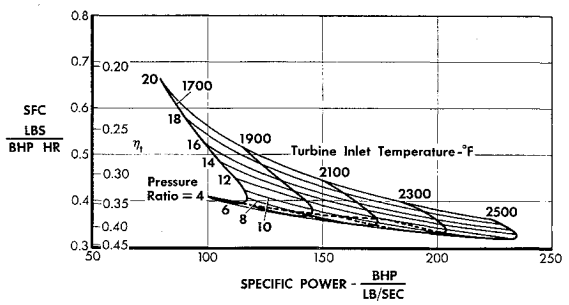

Fig. 39 Regenerative gas turbine performance.

specific fuel consumption. This is a result not only of the increased temperatures but also of the increased compressor pressure ratios that would be used at the higher temperatures. The high specific powers will result in very light engines and the improving specific fuel consumptions will begin to make gas turbine engines competitive with gasoline reciprocating engines and eventually with diesel engines.

Opportunity 29

Large opportunities are available for improving simple-cycle shaft gas turbine performance.

Regenerative Gas Turbines

The simple cycle is not the only available cycle for gas turbines; various forms of reheat, regeneration, intercooling, etc., are possible. Some attention is being given to the simple cycle plus regenerator. Figure 39 is a plot of performance of such engines and is comparable to that on Fig. 38. It is evident that temperature is an extremely important variable in the regenerative cycle and that there is no longer any premium for high compressor pressure ratios. The specific fuel consumptions available with the regenerative cycle are markedly superior to those available from the simple cycle.

Opportunity 30

Regenerative-cycle shaft gas turbines offer marked improvements in SFC over simple-cycle gas turbines.

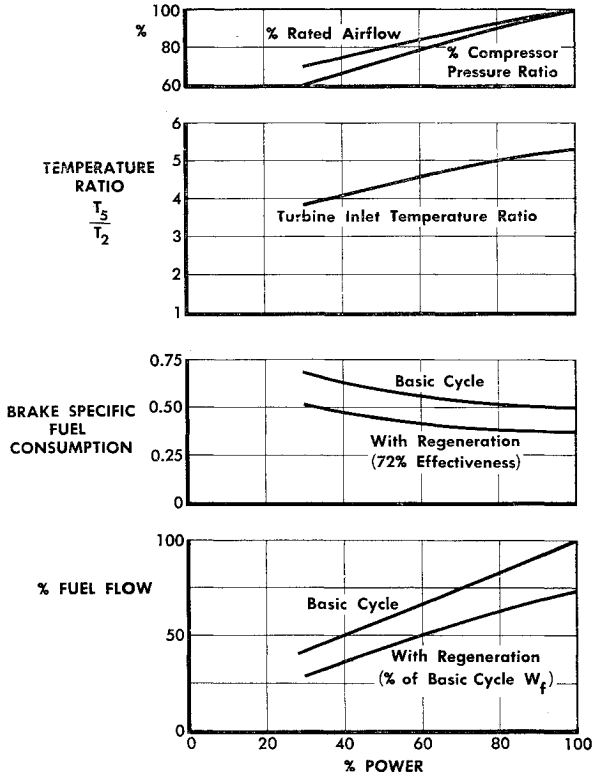

Fig. 40 Part power performance of gas turbines.

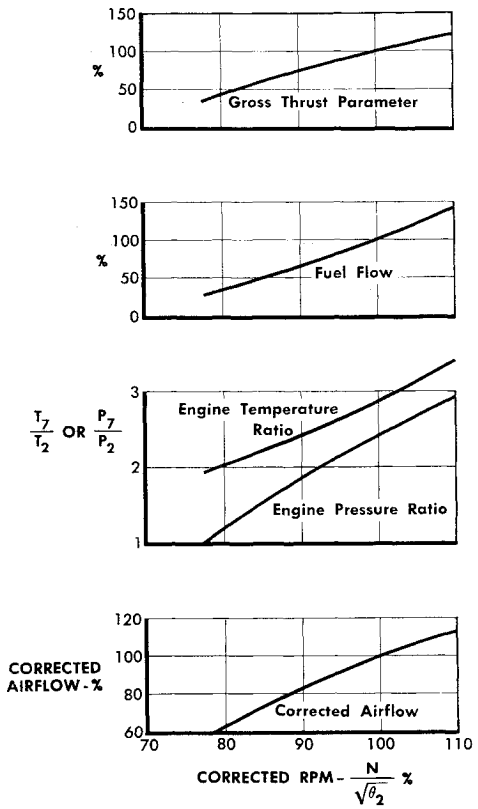

Fig. 41 Turbojet as an air pump.

Off-Design Gas Turbine Performance

In the choice of a gas turbine for an aircraft design, off-design performance will frequently determine the ultimate choice. Figure 40 is a representation of the off-design performance of simple-cycle and regenerative-cycle gas turbines. In order to operate these engines at reduced powers, it was necessary to operate within the limits of airflow vs pressure ratio provided by the compressors. Thus, as shown on Fig. 40, there was only a small reduction in airflow with reducing power, but a marked reduction in pressure ratio, and a very large reduction in turbine inlet temperature. The drop in turbine inlet temperature and pressure ratio cause the large reductions in cycle efficiency. In the particular case chosen, the fuel flow for the regenerative cycle remained at approximately three-quarters of that for the simple-cycle engine regardless of power. These data are typical of the off-design performance of engines, designed with little or no provisions for off-design performance, with the design point at the highest possible power. If a scheme could be evolved by which the engine could operate at high pressure and temperature with reduced airflow, very marked improvements in off-design performance would result. Many schemes for accomplishing this are possible, such as the use of two or more gas generators for each power output turbine. In such a case one or more of the gas generators can be completely shut down and the remaining gas generators operated at full pressure and temperature.

Opportunity 31

Marked improvements in off-design performance of shaft-drive gas turbines are possible by means which reduce the airflow while keeping the temperature and pressure high.

Engine-Airplane Matching

The modern jet transport airplane and the gas turbine engine that powers it have evolved under circumstances which permit a one point design engine to be optimum for both takeoff and cruising. This section will show what is meant by this one design point engine. Figure 41 presents the characteristics of a typical modern turbojet engine as it is seen in the laboratory when tested as an air pump. In this case θ_2 relates to the total temperature in the inlet system. The aerodynamic design of the engine is based on optimum performance at 100% corrected $N/(\theta_2)^{1/2}$; the principal requirement at other rpm's is that the engine shall operate stably and accelerate from one condition to another without stalling.

Figure 41 is the engine as seen by an engine man in an engine laboratory. Figure 42 is exactly the same engine, but the data are as presented by the engine man to the airplane aerodynamics engineer. The thrust is presented as net thrust, with corrections for inlet drag. θ and δ are expressed in terms of atmospheric static temperature and static pressure. At the top of Fig. 42 these same data have been replotted as the efficiency with which the engine converts fuel Btu's into thrust-times-velocity, or power. The dotted line across Fig. 42 shows the conditions under which the corrected rpm at altitude and speed are identical to 100% corrected rpm at static sea-level conditions. At zero velocity at sea level, 100% corrected rpm is the condition for takeoff power. The other crosslines on Fig. 42 are marked to show the maximum power that the engine will provide at varying altitudes for a fixed turbine inlet temperature. The engine designer requires that the engine turbine inlet temperature be somewhat reduced for cruising over that which is allowed for takeoff or maximum power. Hence, cruising thrust must be dropped back somewhat from the maximum thrust shown on Fig. 42, with the net result that at altitude, and with some reduction in temperature for cruising, the maximum allowable cruise power occurs at essentially the same corrected rpm as the maximum allowable takeoff power.

A modern jet transport will have lift-to-drag ratio vs altitude and Mach number relationships, such as those presented on Fig. 43. Also shown on Fig. 43 are lines of constant drag over ambient pressure ratio, T/δ_{AM}, expressed as a percentage of engine-rated thrust. Thus, Fig. 43 presents both airplane efficiency L/D and powerplant thrust requirements T/δ_{AM}. The efficiency of the airplane in converting fuel into transportation is measured by the quantity $L/D \times \eta$, where η is the efficiency with which the powerplant converts fuel Btu's into thrust power and is proportional to $V \div [SFC/(\theta_{AM})^{1/2}]$.

By combining Figs. 42 and 43, optimum cruising circumstances can be found as shown on Fig. 44. Also on Fig. 44, the L/D efficiency of the airplane and the efficiency of the engine when providing the thrust requirements of the airplane are superimposed. Engine efficiency improves with Mach number. At low altitude, airplane L/D is constant with angle of attack, or indicated airspeed, and does not fall

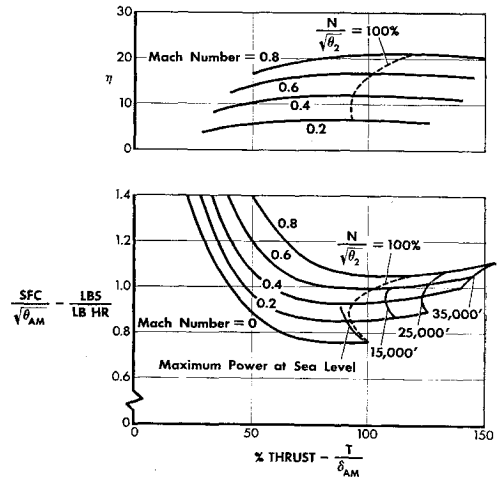

Fig. 42 Turbojet as an aircraft propulsion unit.

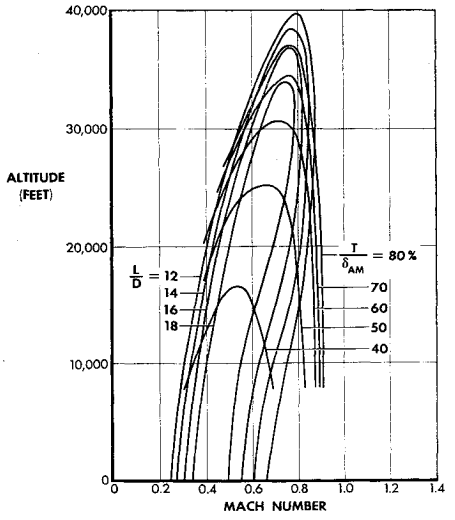

Fig. 43 Subsonic jet transport aerodynamic characteristics.

off until high Mach numbers at high altitudes are reached. The point shown at the top of Fig. 44 is the point at which the maximum product of airplane $L/D \times$ engine η is obtained. Thus, in cruising, the engine is operating at its takeoff design aerodynamic circumstances, and the airplane is at its optimum conditions and under circumstances of speed and altitude that are very attractive to the airline passenger. It is certainly a fortunate coincidence that the modern transport permits the use of a point design engine. These data are for a turbojet, but substantially identical circumstances exist for turbofan engines. The modern jet transport airplane has permitted engine optimization at only one point.

Supersonic Transport

In many applications a single point design engine is not optimum. The basic engine cycle can be modified to provide optimums at several different design points by the use of water injection; afterburning or duct burning; turbofans instead of plain turbojets; variable area nozzles and diaphragms; variable compressor geometry; multiple gas generators for one fan; and many other schemes. Figure 45 presents the lift-drag characteristics of a hypothetical variable-sweep supersonic jet transport. Superimposed in the airplane grid are the over-all powerplant efficiencies of a hypothetical afterburning low-pressure-ratio turbojet engine, such as might be used on a supersonic transport. The peak supersonic and subsonic values of $L/D \times \eta$ are shown on Fig. 45. The four principal design points for the supersonic transport will be takeoff, subsonic cruising efficiency, supersonic cruising efficiency, and transonic acceleration at the highest possible altitude so as to minimize sonic boom. These four points are shown on Fig. 45 and again on Fig. 46, which is a plot of engine specific fuel consumption vs thrust for a number of different Mach numbers.

To optimize the airplane for these four conditions much variable geometry and other special designing is required. During takeoff, the variable sweep wing will be nearly straight and the variable area and camber devices (flaps) will be down to provide a low minimum flight speed and a low drag. The flaps and landing gear are retracted and the variable sweep adjusted to intermediate sweep for subsonic cruising. The wing will be at full sweep and in optimum twist and camber, etc., for supersonic cruising. The wing sweep and area, as well as many wing details, must be optimized to provide the maximum possible altitude capability for transonic acceleration. This is a matter both of minimum drag and also of buffeting, stall, and other lift limitations.

The four principal engine design conditions shown on Fig. 46 require the lowest possible fuel consumptions at subsonic and supersonic cruise thrusts and speeds, the maximum possible thrust in the transonic speed region, and the requirement for adequate takeoff thrust. The takeoff thrust requirement also carries with it a requirement to limit the takeoff noise.

The objective of Figs. 45 and 46 is to point out the multiple design point objectives for both the airplane and engine of the supersonic transport, as contrasted to the simpler circumstances for the subsonic jet transport. Variable geometry is required in the airplane in the form of retractable wing flaps and variable wing sweep. The engines require afterburners with variable nozzles, and possibly silencers, to meet all the different design requirements.

Opportunity 32

The supersonic transport provides engine and airplane designers with incentive to exploit multiple design point systems and variable geometry in both engine and airplane.

Part Power Turbofan Operation

For its weight a modern turbofan engine provides excellent thrust during takeoff and at low speeds. It has good specific fuel consumption at high subsonic Mach numbers. When equipped with a burner, it is an excellent engine at supersonic speeds. The specific fuel consumptions of such engines are quite high at low subsonic Mach numbers, particularly at low percents of maximum thrust. Figure 47 presents specific fuel consumption vs thrust data for a typical turbofan at $M = 0.3$. At the top of Fig. 47 some data are presented on thermal efficiency, propulsive efficiency of the combined fan and jet

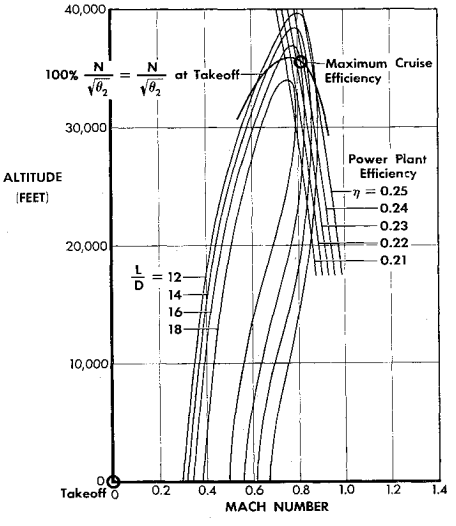

Fig. 44 Matching the aircraft-engine combination.

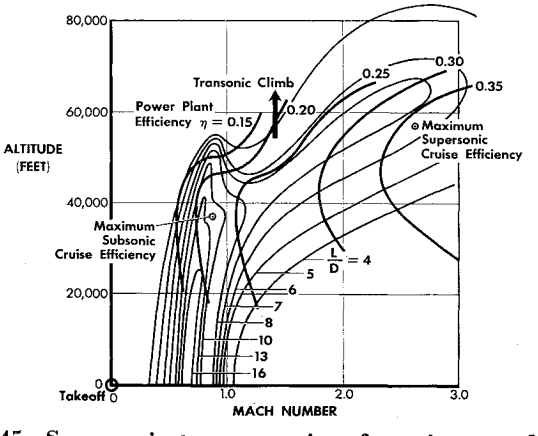

Fig. 45 Supersonic transport aircraft-engine matching.

exhaust air, and over-all efficiency. Thermal efficiency deteriorates very materially as thrust is reduced, but the propulsive efficiency improves.

If such an engine were constructed with one fan and with multiple gas generators, and if these gas generators were shut down in sequence, it would be possible to maintain the thermal efficiency at a high value at any point where the operating gas generators were at full power. The dashed lines on Fig. 47 are an envelope of the conditions that might be obtained by proper choice of a number of declutchable gas generators. The net result of optimum thermal and optimum propulsion efficiencies gives a large possible improvement in specific fuel consumption. This is an envelope of possible conditions and an actual engine might be designed to touch this envelope at only two points rather than all along. Many different ways can be conceived to accomplish the required mechanical changes in an engine to permit operation at maximum thermal efficiency at some one or more reduced power points and, simultaneously, to have the fan operate at maximum propulsive efficiency. If airplane performance requirements were such that an airplane-engine combination must have good characteristics at high subsonic or supersonic speeds and also at reduced power at low Mach numbers, such as cruising or holding at sea level, the added complication and costs of development of an engine, such as suggested on Fig. 47, might well be justified.

Opportunity 33

By the use of ingenuity, and some complication, engine designers can probably find a way to reduce materially the part power, low Mach number, and specific fuel consumption of turbofan power plants.

Vertical Takeoff

A possible requirement for an engine, such as that in Fig. 47, would be in an airplane where range and endurance at sea level are important and where the high-speed requirement was sufficiently high to preclude the use of propellers. This assumed design situation could be further complicated by the assumption that a very high thrust-to-weight ratio was required for takeoff and landing. Figure 48 shows fuel consumption vs thrust performance of a turbofan engine with duct burner and the same engine with the hypothetical improvements of the previous section. Two engine sizes are shown. The large engine represents an engine which would be sufficiently large to provide supersonic operating thrusts without duct burning, but which would have high fuel consumption at part thrust at $M = 0.3$ if the SFC improvements were not included. The large improved engine gives better performance at supersonic speeds than the small engine because afterburning would not be required, and it gives better low-thrust performance because it has a bigger fan.

If the engine were made large enough to provide for vertical takeoff, as in the Hawker P1127, the cruise thrust requirements might be as low as 10% of maximum thrust. It is evident that the fan engine with improved reduced power fuel consumption would entirely change the optimization procedure for design of both engine and airplane in such a case. The takeoff thrust requirement of such a powerplant might well be attained by the supplemental use of special takeoff engines, thus permitting the basic engine maximum thrust requirement to be defined by the high speed condition; the basic engine reduced power conditions to be defined by subsonic endurance and cruising; and the takeoff to be matched by the use of the proper size of added lift engine. The airplane itself would also be subject to optimization by variable sweep, flaps, and other features for the same design points.

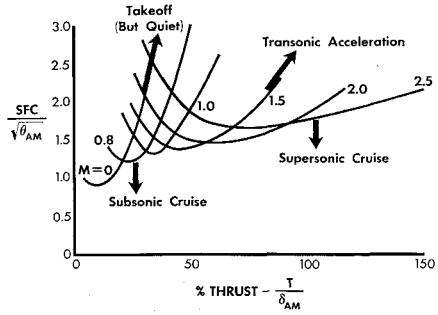

Fig. 46 Supersonic engine specific fuel consumption.

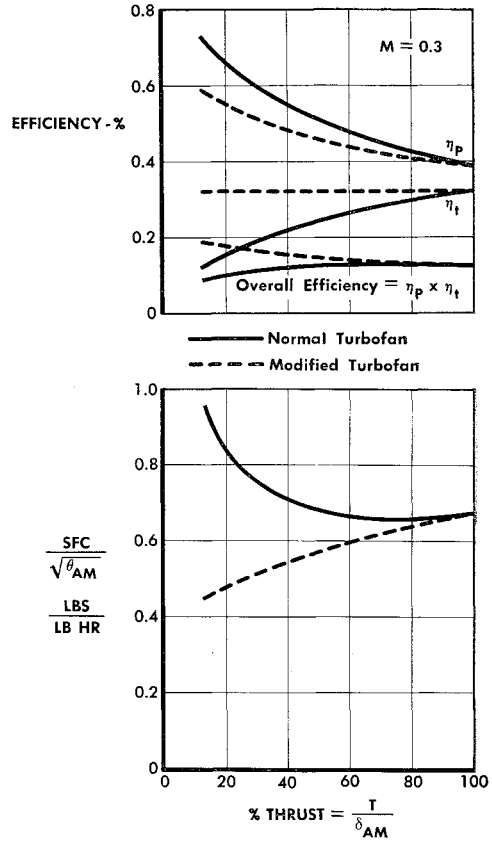

Fig. 47 Part power turbofan performance improvements for $M = 0.3$.

Opportunity 34

The availability of multiple design point engines might entirely change the optimization procedure for low altitude and vertical takeoff aircraft.

Long Endurance

The altitude vs endurance relationship for a modern turbofan commercial transport is shown on Fig. 49. The airplane flies just below the speed for maximum L/D along the maximum endurance line and the maximum L/D improves slowly as altitude is reduced from the altitude for peak endurance. Since the airplane is flying slower as the altitude is reduced, the endurance contribution of the airplane is an increasing function. The fan part of the engine is reduced and should give a further improvement in endurance as the altitude is reduced. Thus the responsibility for the reduction in endurance with reducing altitude lies with the thermal efficiency of the engine. It deteriorates very rapidly with reducing altitude for a number of reasons, including the loss in pressure ratio from ram, the loss in pressure ratio and turbine inlet temperature because the engine is operating at part power, and the loss in thermal efficiency because of the higher inlet temperature. If the thermal efficiency of the engine could be held constant with reducing altitude, the endurance of the airplane would be as shown by the dashed line. En-

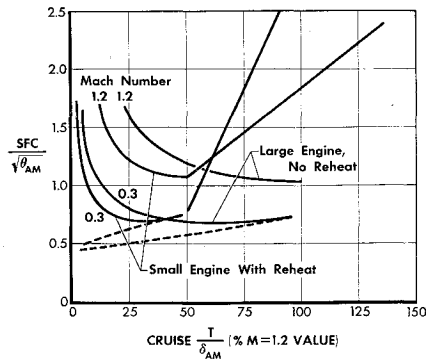

Fig. 48 Specific fuel consumption vs thrust of two sizes of typical duct-burning turbofan engines. Solid lines are for conventional engine; dotted lines are for improved engine of Fig. 47.

gines such as that shown on Fig. 47 could go a long way toward giving such an improvement in endurance at sea level.

If still further improvements in endurance were required, it is conceivable to think of putting a turboprop engine in the the airplane with its size chosen to be just adequate to propel the airplane under maximum endurance conditions at sea level. This engine would be very inadequate for takeoff and altitude cruising and could be supplemented by lightweight high specific fuel consumption lift engines to provide takeoff thrust and altitude operation. If such powerplants were installed in the airplane of Fig. 49, endurances such as those shown might be accomplished. In this case, range and endurance at altitude have been sacrificed to obtain endurance at sea level, but ceiling, takeoff, and high speed at altitude have not been sacrificed.

If the airplane assumed for Fig. 49 were provided with variable sweep, a higher lift-drag ratio would be available at sea level and would provide still greater endurance than shown.

Opportunity 35

Special engine-airplane combinations can provide greatly increased endurance.

Variable Wing Sweep at Altitude

Variable airplane geometry is not a new invention. Retractable landing gears, adjustable stabilizer, retractable flaps, and retractable slats have been used for many years. The development of a requirement and technology for variable-sweep airplane design has come about recently. Figure 50 presents the lift-drag ratio vs Mach number for a high aspect ratio straight-wing airplane, a conventional 35° sweep airplane, a fixed-sweep supersonic transport, and the envelope of conditions possible from a variable-sweep supersonic transport. These data are plotted for optimum L/D with the altitude chosen to provide maximum L/D. It is evident that variable sweep provides nearly optimum altitude L/D at all Mach numbers. Further refinements in aerodynamic design and variable geometry might make possible still further improvements in L/D performance as shown on Fig. 50.

Opportunity 36

Variable geometry permits the airplane to be designed for maximum L/D at altitude at a number of different design Mach numbers.

Variable Geometry at Sea Level

When the airplanes of Fig. 50 are held to sea-level operation, the lift-drag ratios deteriorate to the values shown on Fig. 51. The induced drag becomes negligible at high sea-level Mach numbers and the deterioration in lift-drag ratio with speed is a function of the flat plate drag of the airplane and the supersonic drag rise. Variable sweep is advantageous because it

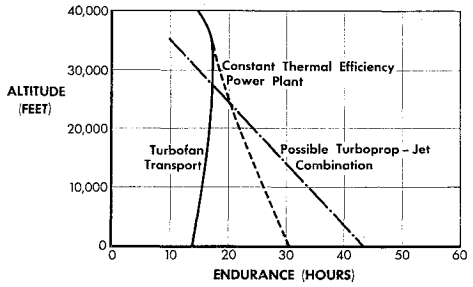

Fig. 49 Altitude endurance of turbofan transport aircraft.

reduces the size of the wings that would be required for low-speed operation and permits these wings to be swept into a low-pressure drag supersonic configuration. Further attention to variable geometry for such aircraft could be directed toward retracting a portion of the wings and tail surfaces to save their wetted drag and by changing their shapes to get more favorable supersonic drag.

Opportunity 37

Variable geometry inventions will probably permit marked improvements in the lift-drag ratios available at sea level at supersonic speeds.

Speed, Range, and Altitude

Three of the principal attributes of aeronautical vehicles are speed, range, and altitude. Figure 52 is a plot of altitude vs Mach number upon which various speed and altitude points can be plotted and labeled with range. The logarithmic scales make it possible to plot satellites, ballistic missiles, and aircraft on the same chart. A number of specific aeronautical vehicles are shown by points or lines as appropriate. These are the 707, the proposed supersonic transport, the X-15, and the re-entry corridor of the Mercury satellite. The flight paths of typical ballistic missiles from apogee down to and through re-entry are shown on Fig. 52. Similarly, a number of possible satellites are shown in terms of perigee and speed at perigee. These data are labeled to show the lifetime of the satellites.

A generalized set of range-speed-altitude data for air-breathing aircraft are shown on Fig. 52. These data are for large aircraft without payload. These data indicate the relative ultimate range possibilities of air-breathing aircraft as a function of altitude and Mach number. The numbers are intended to have relative value only; they would have no significance for any particular practical case other than to indicate the relative difficulty in striving for range at various speeds and altitudes. Maximum range occurs at relatively low speeds and altitudes, and is accomplished by a very highly loaded turboprop airplane. As speed and altitude increase along the maximum range corridor, the maximum possible range drops. There is some loss at the flight conditions of modern commercial transports. There is a sharp drop in

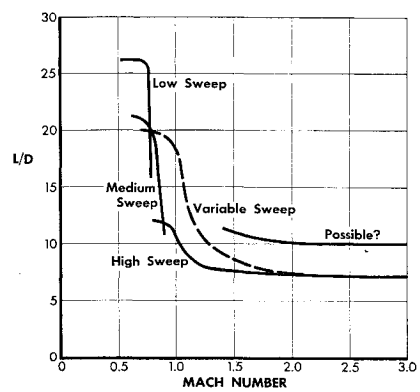

Fig. 50 Cruise altitude lift-to-drag ratios.

ultimate range capability when entering the supersonic speed range. Here the range is relatively constant up to a Mach number of 3, and increases in altitude are required to stay at the maximum range condition. There is a sharp drop in maximum range as the speed is increased at constant altitude at sea level and intermediate altitudes. The ceilings shown on this generalized chart are generally limited by both compressibility drag rise and engine power output. The provision of larger powerplants to provide more power at altitude involves an increase of the weight empty at the expense of the fuel available for range.

Much progress in aviation has come about from speed, altitude, range, and load-carrying record contests. The Schneider Cup Race in England contributed very much to the development of engines, fuel, and aircraft know-how.[48] This made possible aircraft such as the Spitfire, which was so important in World War II. Distance and altitude record attempts through the years have been equally important. Possibly the following records could form the basis for future contests for aircraft with air-breathing powerplants.

1) Maximum range with normal takeoff
2) Maximum range with vertical takeoff
3) Maximum range above Mach 2 with normal takeoff
4) Maximum range above Mach 2 with vertical takeoff
5) Maximum altitude of steady-state flight at subsonic speeds
6) Maximum altitude of steady-state flight at supersonic speeds
7) Maximum range at Mach 2 at sea level with normal takeoff
8) Maximum range at Mach 2 at sea level with vertical takeoff
9) Maximum speed at sea level
10) Maximum speed at altitude
11) Maximum endurance

Opportunity 38

The establishment of a new set of international speed-altitude-range record contests could spur the development of air-breathing aircraft.

Conclusion

All of the progress made in aviation over the last 60 years of flight and the preceding centuries of trying for flight have only sharpened and increased the opportunities for further progress in 1964. A contest for a new set of international records might be a useful spur to further progress. Contests between students at various aeronautical engineering institutions using paper aircraft designs, striving for a different goal in each succeeding year, might be a worthwhile project, both to improve the quality of aeronautical engineering training and to give leadership to aircraft design research.

The material included in this paper is only a very small part of the available data concerning opportunities for further progress in aviation. It is hoped that it will lead others to make similar attempts to state what they do not know and where they think people should search for progress.

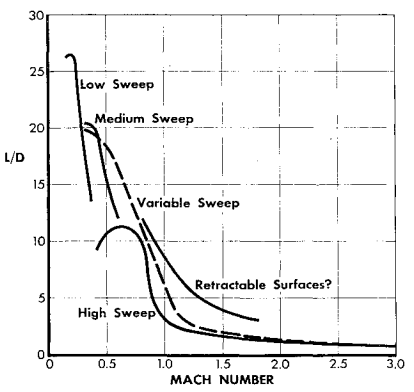

Fig. 51 Sea level lift-to-drag ratios.

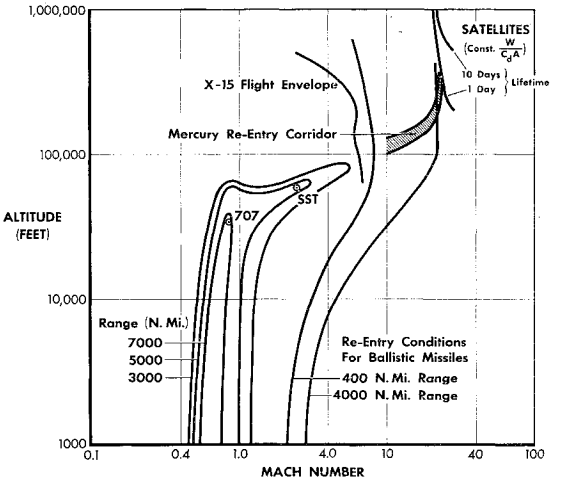

Fig. 52 Aerospace spectrum of speed-altitude-range.

References

[1] Pfenninger, W., "Investigations on reduction of friction on wings, in particular by means of boundary layer suction," NACA Tech. Memo 1181 (August 1947).

[2] Kramer, M. O., "Boundary layer stabilization by distributed damping," J. Am. Soc. Naval Engrs. **72**, 25–30 (February 1960).

[3] Shaver, R. G. and Merrill, E. W., "Turbulent flow of pseudoplastic polymer solutions in straight cylindrical tubes," Am. Inst. Chem. Engrs. Paper **5**, 181–188 (June 1959).

[4] Dodge, D. W. and Metzner, A. B., "Turbulent flow of non-Newtonian systems," Am. Inst. Chem. Engrs. Paper **5**, 189–204 (June 1959).

[5] Carriere, P., Eichelbrenner, E., and Poisson-Quinton, P., "Theoretical and experimental contribution to the study of boundary layer control by blowing," *Advances in Aeronautical Sciences* (Pergamon Press, Inc., London, 1959), Vol. 11, pp. 620–661.

[6] Cornish, J. J., III, "Practical high lift systems using distributed boundary layer control," IAS Preprint 59-18 (1959).

[7] Foley, W. M. and Reid, E. G., "Jet flap thrust recovery," J. Aeronaut. Sci. **26**, 385 (June 1959).

[8] Tsongas, G. A., "Verification and explanation of the controllability of jet flap thrust," Engineer's Thesis, Stanford Univ., SUDAER no. 138 (1962).

[9] Williams, J., Butler, S. F. J., and Wood, M. N., "The aerodynamics of jet flaps," *Advances in Aeronautical Sciences* (Pergamon Press, Inc., London, 1962), Vol. 4, p. 169.

[10] Schlichting, H., "Aerodynamische Problems des Hochsauftriebes," Third International Congress in Aeronautical Sciences, Stockholm, Sweden, Paper ICAS-9 (August 1962).

[11] Kelly, M. W., "Analysis of some parameters used in correlating blowing-type boundary-layer control data," NACA RM A56F12 (September 1956).

[12] Wallace, R. E. and Stalter, J. L., "Systematic, two-dimensional tests of an NACA 23015 airfoil section with a single-slotted flap and circulation control," Municipal Univ. Wichita, Aerodynamic Rept. 120 (August 1954).

[13] Poisson-Quinton, P., "Theoretical and experimental research on boundary layer control," VII° Congres International de Mecanique Appliquee, London (September 1948), Vol. 2, Part II.

[14] Wallis, R. A., "Boundary layer transition at the leading edge of thin wings and its effect on general nose separation," Second International Congress International Council of the Aeronautical Sciences, Zurich, Switzerland (September 1960).

[15] Dannenberg, R. E. and Weiberg, J. A., "Section characteristics of a 10.5 percent thick airfoil with area suction as affected by chordwise distribution of permeability," NACA TN 2847 (December 1952).

[16] Schlichting, H. and Pechau, W., "Lift increase on wings by continuously distributed suction," Z. Flugwissenschaften **7**, 113–119 (1959).

[17] Gersten, K. and Loh, R. R., "Studies on lift increase of wings with simultaneous blowing on the flap of the trailing edge and on the profile nose," Fifth European Aviation Congress, Venice (September 1962).

[18] Wallis, R. D., "Experiments with air jets to control the nose stall on a three-foot chord," NACA BL 4006 Air Force, Dept. Supply Res. Develop. Branch, Aeron. Res. Labs., Australia, Aerodyn. Note 139 (September 1954).

[19] Stratford, B. S., "An experimental flow with zero skin friction throughout its region of pressure rise," J. Fluid Mech. **5**, Part 1, 17–35 (January 1959).

[20] Stratford, B. S., "The prediction of separation of the turbulent boundary layer," J. Fluid Mech. **5**, Part 1, 1–16 (January 1959).

[21] Pearcey, H. H., "The aerodynamic design of section shapes for swept wings," *Advances in Aeronautical Sciences* (Pergamon Press, Inc., London, 1960), Vol. 3, p. 277.

[22] Von Kármán, T., "Tenth Wright Brothers lecture: Supersonic aerodynamics—principles and applications," J. Aeronaut. Sci. **14**, 373–402 (1947).

[23] Von Kármán, T., "The similarity law of transonic flow," J. Math. Phys. **26**, 182–190 (October 1947).

[24] Puckett, A. E. and Stewart, H. J., "Aerodynamic performance of delta wings at supersonic speeds," J. Aeronaut. Sci. **14**, 567–578 (1947).

[25] Bryson, A. E., Jr., "An experimental investigation of transonic flow past two-dimensional wedge and circular arc sections using a Mach-Zehnden interferometer," NACA TN 2560 (November 1951).

[26] Vicenti, W. G. and Wagoner, C. B., "Transonic flow past a double wedge profile with detached bow wave general analytical method and final calculated results," NACA TN 2339 (April 1951).

[27] Vincenti, W. G. and Wagoner, C. B., "Theoretical study of the transonic lift of a double wedge profile with detached bow wave," NACA TN 2832 (December 1952).

[28] Guderly, G. and Yoshihara, H., "The flow over a wedge profile at Mach number one," J. Aeronaut. Sci. **17**, 723–735 (1950).

[29] Busemann, A., "Aerodynamisher Auftrieb bei Überschallgeschwindigkeit," Volta Congress, Rome (1935), German Aeronaut. J. Luftfahart-forschung **12**, 210–220 (1935).

[30] Jones, R. T., "Properties of low-aspect-ratio pointed wings at speeds below and above the speed of sound," NACA Rept. 835 (1946).

[31] Lock, R. C., "The aerodynamic design of swept winged aircraft at transonic and supersonic speeds," J. Roy. Aeronaut. Soc. **67** (June 1963).

[32] Derschmidt, H., "High-speed rotor with blade-lag motion control," IAS Preprint 63-74 (1963).

[33] Durand, W. F. (Ed.) *Aerodynamic Theory* (California Institute of Technology, Calif., reprinted 1944), Vol. II, Div. E, p. 174.

[34] Miller, R. H., "On the computation of airloads acting on rotor blades in forward flight," J. Am. Helicopter Soc. **7**, 56–66 (April 1962).

[35] Helmbold, H. B., "Limitations of circulation lift," J. Aeronaut. Sci. **24**, 237–238 (1957).

[36] Schairer, G. S., "Looking ahead in V/STOL," Eighth Anglo-American Aeronautical Conference, London (September 1961).

[37] Shapiro, J., *Principles of Helicopter Engineering* (Temple Press, Ltd., London, 1955), p. 17.

[38] Spence, D. A., "The lift on a thin airfoil with a jet-augmented flap," Aeronaut. Quart. **9**, 287–299 (1958).

[39] Spence, D. A., "Some simple results for two-dimensional jet-flap aerofoils," Aeronaut. Quart. **9**, 395–406 (1958).

[40] Yoler, Y. A., "A lifting line theory of the jet flapped wing," Boeing Sci. Res. Labs. Doc. D1-82-0042 (January 1960).

[41] Maskell, E. C. and Spence, D. A., "A theory of the jet flap in three dimensions," Royal Aircraft Establishment Rept. Aero 2612, Ministry of Supply, London, W.C.2.

[42] Davidson, I. M., "The jet flap," J. Roy. Aeronaut. Soc. **60**, 25–41 (January 1956).

[43] Smelt, R. and Davies, H., "Estimation of the increase of lift due to slipstream," Ames Research Center, Res. and Develop. 1788 (1937).

[44] Mitchell, R. G., "Full-scale wind tunnel test of the VZ-2 airplane with particular reference to the wing stall phenomena," NASA TN D-2013 (December 1963).

[45] Anonymous, "Breguet 941, un avion sain," Air et Cosmos, Paris (October 1963).

[46] Delano, J. B. and Carmel, M. M., "Investigation of the NACA 4-(5) (08)-03 two blade propeller at forward Mach numbers to 0.925," NACA RM L9G06a (September 1949).

[47] Maynard, J. D., Swihart, J. M., and Norton, H. T., Jr., "Effects of blade section camber on aerodynamic characteristics of full scalle supersonic type propellers at Mach numbers to 1.04," NACA RM L36E10 (October 1956).

[48] Schlaifer, R. and Heron, S. E., *Development of Aircraft Engines and Fuels* (Andover Press, Harvard Univ., Mass., 1950).